DESY Photon Science Users' Meeting 2023
European XFEL Users' Meeting 2023

Jointly organized Users' Meeting of
DESY Photon Science and European XFEL

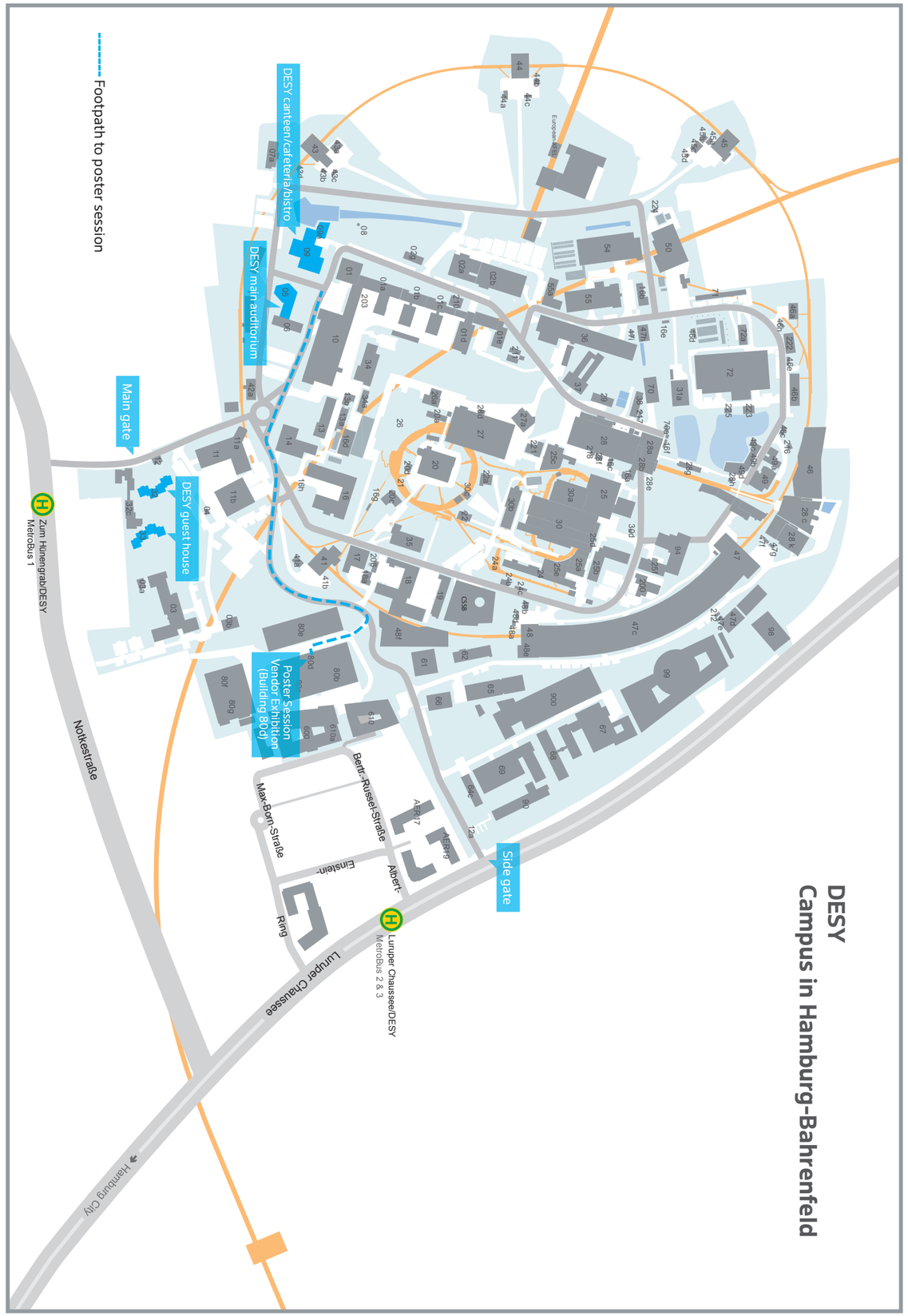

DESY Photon Science User Committee (DPS-UC)

Election 2023

Please vote ✗ online until

Wednesday, 25 January, 15 h

door.desy.de

All active users eligible to vote have received a corresponding e-mail.

(DESY on-site staff is not eligible to vote)

DESY Photon Science Users' Meeting 2023
European XFEL Users' Meeting 2023

January 2023 in Hamburg

DESY Auditorium (Bldg. 5)

Monday, 23 January: Satellite Workshops

09:00 – 19:00	High Rep Rate Fixed Target Delivery: Chip standardisation and workflow	**European XFEL** | Room E1.173
09:00 – 17:00	X-ray Raman and other non-resonant Inelastic X-ray Scattering at XFELs	**DESY** | Building 15, CSSB Auditorium,
13:00 - 17:00	Data analysis at FLASH	**DESY** |Building 28c, SemR FLASH
10:00 - 18:15	FLASH THz User Workshop	**DESY** | Building 99, CFEL I

Tuesday, 24 January: Satellite Workshops

09:00 - 17:00	Advanced X-ray Instrumentation, Optics and Metrology	**DESY** |Building 28c, SemR FLASH
13:00 - 17:00	Status of the HED instrument and the HIBEF contributions and scientific highlights	**European XFEL** | Room E1.173
14:00 - 17:00	Computing for Photon Science	**DESY** | Building 15, CSSB Auditorium,
09:15 - 17:00	Momentum Microscopy at FLASH and PETRA III	**DESY** | Building 99, CFEL I**II**
08:30 - 12:30	ExPaNDS workshop: Open Data for Open Science	**DESY** | Building 1b, SemR 4a+b
09:00 - 18.00	Present and future opportunities for the investigation of gas-phase biomolecules at FEL and SR facilities	**DESY** | Building 99, CFEL I**I**

Wednesday, 25 January 2023: European XFEL Users' meeting - Plenary Sessions

08:30–10:00	**Registration**		
10:00-10:20	**Opening session**		
10:00	Welcome	R. Feidenhans'l	*European XFEL*
10:10	Opening adress from the Council Chair	F. Boscherini	*U Bologna*
10:20-12:45	**European XFEL Update Session**		*Chair: S. Molodtsov*
10:20	General status of the project	R. Feidenhans'l	*European XFEL*
11:00	Accelerator and FEL Sources- Status and Future Plans	W. Decking	*DESY*
11:30	Handling Petabyte Data Sets at European XFEL: Updates on Policy and Implementation	S. Aplin	*European XFEL*
12:00	News from the European XFEL User Organisation and Bestowal of the Young Scientist Award	A. Eschenlohr	*U Duisburg-Essen*
12:15	Young Scientist talk		
12:45–14:00	**L u n c h b r e a k**		

14:00-15:30 Science Session I

Chair: S. Bajt

14:00	Time-resolved RIXS of NiO photoexcited above the optical gap	L. Martinelli	*PoliM*
14:30	XFEL MHz imaging study ultrasonic liquid phase exfoliation of 2D materials	J. Mi	*U Hull*
15:00	Ultrafast structural dynamics in metal complex photosensitisers and catalysts	J. Weinstein	*U Sheffield*
15:30-16.00	**Coffee break**		

16:00-17:10 Science Session II

Chair: M. Naumova

16:00	Simultaneous X-ray emission spectroscopy and diffraction from pressurized matter during X-ray heating	C. Sternemann	*TU Dortmund*
16:30	Dynamics of Nanoplasma Expansion in Spherical and Fibrous Nanoparticles	E. Rühl	*FU Berlin*
17.00	New regimes of nuclear resonance exitation at the European XFEL	R. Röhlsberger	*U Jena*
17.30 – 20.30	Scientific POSTER Session & Vendor Exhibition (Part 1 - European XFEL/FLASH/external/theory/other) with Fingerfood & Refreshments		**Building 80d, DESY**

Thursday, 26 January: DESY Photon Science Users' Meeting - FLASH

Chair: E. Ploenjes

9:00-9:10	Welcome - FLASH session	E. Weckert	*DESY*
9:00-9:40	FLASH Strategy	M. Gühr	*DESY*
9:40-10:10	Status FLASH2020+ project	L. Scharper	*DESY*
10:10-10:40	**Coffee break**		

Chair: R. Treusch

10:40-11:10	Time- and channel-resolved inner-shell photoelectron spectroscopy	F. Allum	*SLAC Stanford, USA*
11:10-11:40	Mixing laser- and X-ray-beams for probing the electronic structure of solids by non-linear spectroscopy	D. Schick	*MBI Berlin*
11:40-12:10	Fragmentation dynamics of polycyclic aromatic hydrocarbons explored using ultrafast XUV-Vis and XUV-IR pump-probe spectroscopy	M. Schnell	*DESY/CAU Kiel*
12:10-12:40	Ultrafast and wavelength-tunable ytterbium lasers for FEL science and electron acceleration	C. Heyl	*DESY/Univ. Jena*
12:40-14:00	**Lunch break**		

Science Session: Soft X-ray FEL Science Highlights (jointly organised)

Chair: A. Eschenlohr

14:00-14:30	Distinguishing Molecular Isomers by XFEL-based 3-D Coulomb Explosion Imaging	D. Rolles	*U Kansas State*
14:30-15:00	Exploring Funamental electron dynamics with attosecond X-ray pulses	M. Ilchen	*DESY*
15:00-15:10	Report of the ´European synchrotron and FEL user organisation´ (ESUO)	C. McGuinness	*Trinity College, Dublin*

15:10-15:40	**Coffee break**		
15:40-16:10	The ultrafast interfacial movie- imagining electronic and structural dynamics at the space- time limit	K. Baumgärtner	*U Würzburg*
16:10-16:40	Controlling x-ray mattter interaction by collision-induced changes of electronic populations	A. Benediktovitch	*U Hamburg*
17:00-20:30	Scientific POSTER Session & Vendor Exhibition (Part 2 - PETRA III / PETRA IV) with Fingerfood & Refreshments		**Building 80d, DESY**

Satellite workshops

11:00 - 17:00	13th Workshop on X-Ray Nano-Imaging of Biological and Chemical Systems at PETRA III	**DESY** | Bldg. 99, CFEL Sem. R. I-III
11:00 - 17:00	SAXS/WAXS/GISAXS@DESY	**DESY** |Building 28c, SemR FLASH
13:00 - 17:00	High Energy X-ray Diffraction for Physics and Chemistry	**DESY |** Building 1b, SemR 4a+b
9:00 - 12:00	The Swedish Materials Science beamline at PETRA III	**DESY |** Building 25f, SemR 456
13:00 -18:30	Status and research highlights of the ECB (P2.02) at PETRA III	**DESY |** Building 25b, SemR 109
13:00 - 16:30	In situ studies at extreme conditions using the Large Volume Press at P61B	**DESY |** Building 48f/O1.030
13:00 - 17:00	High-pressure photoemission at POLARIS: catalysis at industrially relevant conditions	**DESY |** Building 47c/110
11:00 - 18:00	X-Ray Absorption Spectroscopy today and perspectives for future PETRA III and IV beamlines	**DESY |** Building BAH I+II
14:00 - 16:00	Accelerators as Innovation Boosters: Presenting the Innovation Platform HI-ACTS for easy and efficient use of accelerator technologies across industries	tba
13:00 - 17:30	GEMS Satellite Meeting	Bldg. 94 SemR 01.1041

Friday, January 27: DESY Photon Science Users' Meeting 2023

8:30 – 9:00	**Registration**		
			Chair: K. Rossnagel
09:00-9:15	Welcome	H. Dosch	*DESY*
09:15-9:45	Overview DESY Photon Science	E. Weckert	*DESY*
09:45-10:15	PETRA III	C. Schroer	*DESY/U Hamburg*
10:15 - 10:45	**Coffee break**		
			Chair: H.-C. Wille
10:45-11:30	PETRA IV Upgrade Project	H. Reichert	*DESY*
11:30-12:00	PETRA IV Beamline Portfolio	K. Bagschik	*DESY*
12:00-12:15	Report of the Desy Photon Science User Committee (DPS-UC) - Results of Election	P. Mueller-Buschbaum	*TU München*
12:15-12:25	Research with Photons - Light for the Future: News from the KFS (Comittee Research with Synchrotron Radiation)	J.-D. Grundwaldt	*KIT Karlsruhe*
13.10 - 14:00	**Lunch break**		

Chair: S. Techert

13:30-14:00	Manipulation of host cells by infecting bacteria	A. Itzen	*UHH, UKE*
14:00-14:30	The state of zinc in methanol synthesis over a Zn/ZnO/Cu(211) model catalyst	P. Amann	*U Stockholm*
14:30-15:00	Use of AI for synchrotron data analysis	T. Strohmann	*DLR*
15:00-15:30	DAPHNE	B. Murphy	*CAU*

Satellite workshops

15:30 - 19:00	LifeScience&Health@DESY – From presence to future A new approach for high-impact biomedical research at DESY	DESY | Bldg. 28c SemR FLASH
10:00 - 16:30	Data analysis at the European XFEL	Online

General Information

Main sessions and coffee breaks

The **mains sessions** will be held in the DESY Auditorium (Bldg. 5). The **coffee breaks** will not take place in the auditorium foyer, but in the more spacious DESY cantine (Bldg. 9), directly opposite to the DESY Auditorium.

Poster sessions with light dinner

The poster sessions on Wednesday and Thursday afternoon will take place in Bldg. 80d. This big hall is located on the DESY campus close to the PETRA III experimental hall 'Ada Yonath' (Bldg. 48f) and near to the side gate: Luruper Chaussee 149, 22761 Hamburg (see map).

Wednesday, 25 January, 17:30-20:30h
Scientific poster session (Part 1 -mainly FEL Science)
with fingerfood & refreshments (European XFEL)

Thursday, 26 January, 17:00-20:30h
Scientific poster session (Part 2 - mainly SR Science)
with fingerfood & refreshments (DESY Photon Science)

Vendor exhibitions

The vendor exhibitions will take place in the same Bldg. 80d in parallel to the scientific poster sessions. Vendor exhibition starts at 15:00h.

WLAN

Science-Hotspot
This guest WLAN does not require user registration. Users only have to accept the usage regulations on the portal website of the WLAN network.

eduroam
For guests, whose home institutes are participating in the project eduroam, we offer this wireless guest network connection.

Organizers

S. Bertini (European XFEL), K. Baranašić (European XFEL), Gabriela Heeßel (European XFEL), M. Kreuzeder (DESY), K. Kucza (DESY), W. Laasch (DESY), F. Lehmkühler (DESY), S. Molodtsov (European XFEL), Giulia Quondam (European XFEL), A. Rothkirch (DESY), D. Unger (DESY)

Local Information

Meals

Breakfast
If you stay at the DESY guest house you may have breakfast in the DESY cafeteria (opens at 07:00, Bldg. 9) or CFEL Cafeteria (opens at 8:00, Bldg. 99) at your own expenses.

Lunch
You may have lunch in the DESY canteen (Bldg. 9) or CFEL Cafeteria (Bldg. 99) at your own expenses.

Public Transportation

Bus (HVV): Bus stops near the main entrance: 'Zum Hünengrab (DESY)' and near the side entrance: 'Luruper Chaussee (DESY)'. Further information: www.hvv.de

Bike rental (StadtRAD Hamburg): Two city bike stations are on the DESY campus where bikes can be returned. Further information: stadtrad.hamburg.de

Online Information

Programme workshops, etc.

Link : https://indico.desy.de/event/36974/

ABSTRACTS

News from the European XFEL User Organisation and Bestowal of the Young Scientist Award

Andrea Eschenlohr

Faculty of Physics and Center for Nanointegration Duisburg-Essen (CENIDE),
University Duisburg-Essen, 47048 Duisburg, Germany

I will present a review of the activities of the European XFEL User Organisation during 2022, including the results of our recent User Survey, and discuss our plans for 2023. New members of the organisation‘s Executive Committee who were recently elected will further be introduced.

The presentation will be followed by the bestowal of this year’s Young Scientist Award, which includes a scientific talk by the award winner.

Time-resolved RIXS of NiO photoexcited above the optical gap

Martinelli L.[7], Adriano L.[1], Alic A.[2], Baykusheva D. R.[13], Carley R.[1], Chiuzbaian G.S.[2], Dean M. P. M.[3], Duros O.[2], Foelisch A.[4], Foerst M.[5], Freelon B.K.[6], Gerasimova N.[1], Ghiringhelli G.[7], Jiang X.[9], Jost D.[9], Kusch M.[4], Laarman T[10], Lebedev V.[11], Lee W.S.[9], Liu C.Y.[4], Mercadier L.[1], Merzoni, G.[1,7], Minola M.[12], Mitrano M.[13], Molodtsov S.[1], Pathiraja C.S.[6], Parchenko S.[1], Ranhili Pelige J.N.[6], Peng Y.[8], Qiu Q.[8], Schmitt T.[14], Sears J.[3], Scherz A.[1], Sreenkatan Nair Lalithambika S.[10], Techert S.[10], Teichmann M.[1], TenHuisen S. F. R.[13], van Kuiken B.[1], Yin Z.[1], Schlappa J[1].

[1]European XFEL, Schenefeld, Germany
[2]Sorbonne University, Laboratoire de Chimie Physique-Matière et Rayonnement, Paris, France
[3]Brookhaven National Laboratory (BNL), Upton, NY, United States
[4]Helmholtz-Zentrum Berlin für Materialien und Energie GmbH, Berlin, Germany
[5]Max-Planck-Institut (MPI) für Struktur und Dynamik der Materie (MSPD), Germany
[6]Department of Physics and Texas Center for Superconductivity, University of Houston, Houston, TX
[7]Dipartimento di Fisica, Politecnico di Milano, Milano, Italy
[8]International Center for Quantum Materials, School of Physics, Peking University, Beijing, China
[9]Stanford University and SLAC, SIMES, Stanford, United States
[10]Deutsches Elektronen-Synchrotron DESY, Hamburg, Germany
[11]Bernal Institute, University of Limerick, Limerick, V94 T9PX, Ireland
[12]Max Planck Institute for Solid State Research, Solid State Spectroscopy, Stuttgart, Germany
[13]Harvard University, Department of Physics, Cambridge, MA, United States
[14]Paul Scherrer Institut, Laboratory Condensed Matter, Villigen-PSI, Switzerland

Ultrafast pump-probe techniques have become a fundamental tool in condensed matter physics. The development of a high resolution x-ray absorption (XAS) and resonant inelastic x-ray scattering (RIXS) instrument at the SCS beamline of the European XFEL is a cornerstone in the field of time resolved x-ray techniques. For the commissioning of the Heisenberg RIXS (hRIXS) spectrometer, we carried out the first pump-probe (pp) RIXS measurements at SCS.

As a test case we have selected NiO, one of the prominent examples of strongly-correlated materials, with a mixed charge-transfer and Mott-Hubbard gap of almost 4 eV and 3D antiferromagnetism. Recent time-resolved photoemission experiments have discovered an intriguing coupling between the electronic excitations and the magnetic order, and found rather long-lived coherent oscillations between many-body states [1]. The goal was to study how the magnetic and orbital excitations evolve in response to the photoexcitation of electrons above the optical gap.

We measured time-resolved XAS and RIXS of NiO at the nickel L_3 edge (853 eV), with a 266 nm (4.6 eV) laser pump, a temporal resolution of ≈100 fs and a combined energy resolution of ≈ 80 meV. We acquired spectra changing the pump delay between 0.1 ps and 50 ps, and the laser fluence on the sample from 1 mJ/cm^2 up to 35 mJ/cm^2.

We have found a clear and long-lived broadening and energy-shift of the crystal field excitations, possibly caused by thermal expansion of the crystal. At the same time, we have found evidence in the XAS of a meta-stable state, visible in the XAS spectrum as new resonance emerging 1.2 eV below the main Ni^{2+} edge. RIXS spectra measured at this incident energy reveal a pair of Stokes – Anti-Stokes peaks sitting around $\pm$0.7 eV, disappearing with a dynamics of about 2 ps. Other modifications to the RIXS spectra, mostly in the quasielastic region and at the main orbital excitation peak, persist over a longer time scale of tens of picoseconds. The analysis and interpretation of these data is still ongoing. However, it seems quite evident that the optical pump generates in NiO a relatively long-lived excitonic state that decays into more delocalized electronic excitations. The potential of ppRIXS is here demonstrated, because the assignment of spectra features is straightforward, the transient modifications to the spectra are very large and the measurements are relatively quick.

References

[1] Gillmeister, Konrad, et al. "Ultrafast coupled charge and spin dynamics in strongly correlated NiO." *Nature communications* 11.1 (2020): 1-9.

XFEL MHz imaging study of ultrasonic liquid phase exfoliation of 2D materials

Jiawei Mi

School of Engineering, University of Hull, UK

Ultrasonic liquid phase exfoliation is a promising manufacturing route for 2D functional materials. In the applied ultrasonic fields within the different liquid media used, the oscillating and imploding ultrasonic bubbles play critical roles in enabling 2D layer exfoliation. The highly transient phenomena occur at μm length scale and sub-μs time scale. It is very difficult to observe in real-time these highly dynamic phenomena in operando conditions. Hence many fundamental issues in the ultrasonic liquid phase exfoliation processes have not been fully understood or not fully quantified. In 15th-19th September 2022, we conducted the first official megahertz imaging user experiment at the SPB/SFX beamline of the European XFEL. The unique world leading XFEL imaging capability (20 KeV, 10 Hz pulse trains with 1.13 MHz repetition rate) allows us to observe directly the highly transient phenomena of bubble implosion and shock wave generation in different liquid media under different ultrasound conditions. The exfoliation of bulk graphite into 2D nano/micro layers and their growth dynamics were quantified for the first time *in situ*. The discoveries pay the way for further optimization of the ultrasonic liquid phase exfoliation processes for different types of 2D functional materials.

Ultrafast structural dynamics in metal complex photosensitisers and catalysts:
Femtosecond X-ray Emission study of the excited state pathway in a photo-antibacterial copper complex – what comes first, intersystem crossing or structural change?

Rory A. Cowin, Martin V. Appleby, Iona Ivalo, Catherine Royle, Julia A. Weinstein
Department of Chemistry, the University of Sheffield, Sheffield S3 7HF, UK. Julia.Weinstein@Sheffield.ac.uk
Frederico Lima, Chris Milne, Yohei Uemura, Mykola Biednov, Dmitry Khakhulin
EU XFEL, Hamburg, Germany

Transition metal (TMC) complexes have been widely used in light-driven applications such as artificial photosynthesis, catalysis and photodynamic therapies, for decades. TMC owe such success to desirable photophysical properties: (i) tuneable light absorption across the visible range via modification of the ligands which change the energy of the Metal-to-Ligand Charge transfer (MLCT) state; (ii) the lowest triplet excited state, ^{3}MLCT is efficiently populated *via* ultrafast intersystem crossing (ISC). (iii) the long, >100 ns, lifetime of the triplet state enables efficient bimolecular reactions in e.g. photocatalysis or singlet oxygen ($^1O_2$) generation.

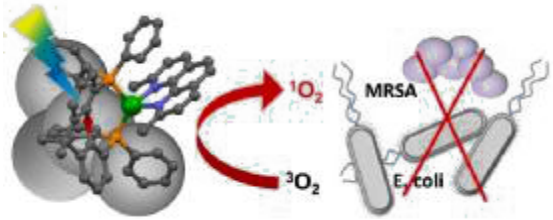

Figure 1. *A cartoon representation of **Cu1** complex under 405 nm light killing Gram-negative E.Coli and Gram-positive MRSA bacteria.[1] Sngle crystal X-ray diffraction data: Green - Cu, blue – N, orange – P, red – O. H-atoms omitted.*

Tetracoordinate Cu(I) complexes [2-6], where the lowest electronic excited state is of MLCT character, have shown promise as a replacement for the typically used complexes of rare metals (Ru, Pt) as photosensitisers in applications such as antibacterial water purification. However, Cu(I) *homoleptic* diimine complexes often have excited state lifetimes too short for efficient bimolecular reactions, due to geometric distortion upon photoexciation from the pseudo-tetrahedral ground-state geometry to the pseudo square-planar configuration in the MLCT excited state. In these homoleptic complexes, sterically hindering ligands are employed to prevent this distortion and thus increase the lifetime of the excited state.

We have recently demonstrated a representative of a class of heteroleptic **Cu(PP)(NN)** complexes, containing one diimine ligand and one di-phosphine ligand (Fig 1, PP = xanthphos, NN = 2,9-dimethyl-phenanthroline) as the first example of a Cu(I) complex as an efficient photo-antibacterial agent due to a relatively long excited state lifetime of ~200 ns.[1] Synchrotron-based studies of similar **Cu(NN)(PP)** complexes revealed changes in Cu-P and Cu-N bond-length on the >80 ps time-range.[7]

To better understand the photophysical properties of this class of complexes, early time evolution of structural, electronic, and spin dynamics needs to be investigated. The information obtained from femtosecond XES studies at the FXE beamline (Fig. 2) will be discussed. The XES data are complemented by femto-second electronic transient absorption and fluorescence upconversion data on **Cu(NN)(PP)** complexes with various degree of steric hindrance, that indicate the presence of sub-10 ps processes in solution.

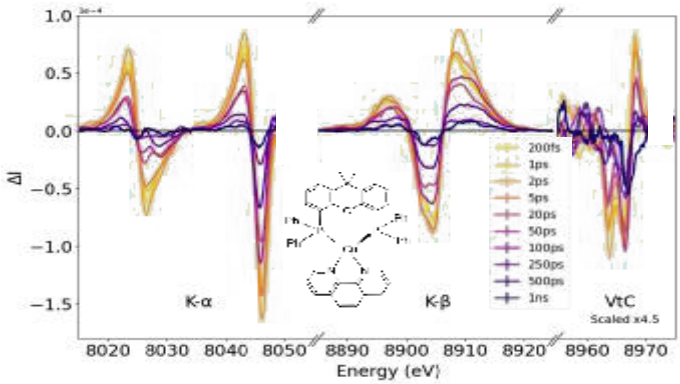

Figure 2. X-ray emission data, FXE beamline, 2022. Excitation 400 nm, 20 mM solution of [Cu(PP)(NN)][BF_4] in acetonitrile.

The mechanism of the excited state decay, including a competition between ISC and structural distortion in heteroleptic Cu(I) complexes is proposed, based on the ultrafast FXE data and optical data and complemented by TDDFT calculations. Complementary X-ray and optical data are a starting point for a wider systematic investigation into the fundamental mechanism of ISC in transition metal complexes.

We thank EU XFEL for the beam time, EPSRC UK for funding the Lord Porter Laser Laboratory in Sheffield and PhD studentship (I.I.); UK XFEL Physical Sciences hub (PhD studentship for R.A.C), the Grantham Center (M.V.A.); the University of Sheffield; and Prof P Wernet, Prof W Gawelda, Prof T Katayama for discussions.

1. Appleby et al, *Materials Advances* 2020, **1**, 3417; 2. Penfold et al. *Chem. Rev.* 2018, **118**, 6975,
3. Katayama et al, *Nature Comm*., 2019, **10**, Article number: 3606.
4. Potochny et al, *Inorg. Chem.*, 2022, 19119; 5. Iwamura et al. Acc. Chem. Res. 2015, 48, 782.
6. Katayama et al, 2022, https://chemrxiv.org/engage/chemrxiv/article-details/6389591a836ceb164c6f8788
7. Rentschler et al, *Chem. Eur.J*. 2020, **26**, 9527.

Simultaneous X-ray emission spectroscopy and diffraction from pressurized matter during X-ray heating

Christian Sternemann

Fakultät Physik / DELTA
Technischer Universität Dortmund
D-44221 Dortmund, Germany

christian.sternemann@tu-dortmund.de

The investigation of the electronic state of matter at extreme conditions using X-ray spectroscopy became feasible using diamond anvil cell technology coupled to laser-heating devices or shock compression experiments. This way one can achieve conditions of planetary interior in the laboratory, i.e. for example about 136 GPa and 3000 K for the core-mantle boundary of our planet. Only recently X-ray heating was exploited as an alternative approach to heat a sample contained in a diamond anvil cell. Here, femtosecond X-ray pulses from an X-ray free electron laser (XFEL) source are used to heat the material and to probe the hot state under static compression by the same X-ray pulse train. This method was so far predominantly combined with X-ray diffraction. In order to extend such studies to spectroscopic applications, we implemented a von Hámos type spectrometer in the interaction chamber 1 of the High Energy Density (HED) instrument of the European XFEL. This setup allows to study the electronic state of a sample at high-temperature and high-pressure using K_β X-ray emission of e.g. transition metals in the 6 to 11 keV range and can be combined with simultaneous X-ray diffraction. It can be also applied to measure valence-to-core emission spectra as well as to conduct inelastic X-ray scattering experiments with an energy resolution in the 1-eV range. The implementation and commissioning of the spectrometer will be presented and examples for the study of high-pressure high-temperature states of iron in $FeCO_3$ and FeS will be discussed. Future applications of the high-resolution von Hámos spectrometer at the HED instrument are not limited to the study of samples with X-ray heating but can be extended to e.g. laser-pump X-ray probe and laser driven shock compression experiments.

Dynamics of Nanoplasma Expansion in Spherical and Fibrous Nanoparticles

F. Gerke[1], P. Tümmler[2], S. Biswas[3], S. Dold[4], D. Rivas[4], T. Baumann[4], B. Kruse[2], L. Seiffert[2], T. Mullins[4], P. Grychtol[4], Y. Ovcharenko[4], B. Wassermann[1], S. Rafie-Zinedine[4], M. Meyer[4], A. Maity[5], V. Polshettiwar[5], M. F. Kling[3], C. Peltz[2], T. Fennel[2], and E. Rühl[1]

[1] Physical Chemistry, Freie Universität Berlin, Arnimallee 22, 14195 Berlin, Germany
[2] Institute of Physics, University of Rostock, 18051 Rostock, Germany
[3] Physics Department, Ludwig-Maximilians-Universität Munich, 85748 Garching, Germany
[4] European XFEL, Holzkoppel 4, 22869 Schenefeld, Germany
[5] Department of Chemical Sciences, Tata Institute of Fundamental Research, Mumbai, 400005, India

The ultrafast nanoplasma dynamics of spherical[1] and fibrous[2] silica nanoparticles probed by X-rays from the SASE3 soft X-ray undulator at the European XFEL at the SQS instrument is reported. Isolated nanoparticles were prepared in an aerodynamically focused beam that was excited by pulsed infrared radiation at 800 nm (1 mJ/pulse, 188 kHz, 20 fs duration) synchronized to pulsed soft X-rays of 1 keV photon energy, 25 fs pulse duration, and an energy of 7 mJ per pulse in the NQS chamber. The scattered X-rays are monitored by a pnCCD-detector. Systematic studies involving infrared-pump-X-ray-probe experiments with delays of the X-rays reaching up to 15 ps reveal ultrafast processes involving the dynamics of temporary surface melting of spherical particles as well as irreversible changes of the particle's surface structure, most prominently observed for fibrous nanoparticles. This goes beyond recent results focusing on the femtosecond dynamics of spherical silica nanoparticles.[3] Distinct importance for these dynamical processes has the polarization of the radiation fields. This is evidenced by different observables, such as the delay-dependent slope of the scattered X-rays as a function of the scattering wave vector and the asymmetry of the scattering patterns. Modeling the experimental results by molecular dynamics simulations leads to new insights into the nanoplasma dynamics as a function of nanoparticle shape as well as reversible and irreversible plasma-induced structural changes of the nanoparticles.

References

1. E. Antonsson et al., J. Chem. Phys. **146**, 244301 (2017).
2. V. Polshettiwar, Acc. Chem. Res. **55**, 1395 (2022).
3. C. Peltz et al., New J. Phys. **24**, 043024 (2022).

New Regimes of Nuclear Resonance Excitation at the European XFEL

Ralf Röhlsberger for the MCLS* collaboration and for the ^{45}Sc collaboration

Helmholtz Institut Jena, Fröbelstieg 3, 07743 Jena, Germany
Friedrich-Schiller-Universität Jena, Max-Wien-Platz 1, 07743 Jena, Germany
Deutsches Elektronen-Synchrotron DESY, Notkestr. 85, 22607 Hamburg, Germany

The nuclear resonances of Mössbauer isotopes provide extremely narrow energy references for high-resolution spectroscopy. This qualifies them for applications in condensed matter physics as well as for studies in fundamental physics and extreme metrology. Since the pioneering experiment by E. Gerdau et al. [1] at the storage ring DORIS (DESY, Hamburg), the technique of nuclear resonance scattering has found widespread applications at hard X-ray synchrotron radiation sources worldwide. Its implementation and use at hard X-ray laser sources started with one experiment performed at SACLA in Japan reported so far [2].

Science with nuclear resonances at the European XFEL commenced in 2022 with two experiments to be reported here. One study was conducted at the 14.4 keV resonance of ^{57}Fe aiming at applications in x-ray quantum optics [3], the other experiment resulted in the first-time photonic excitation of the ultranarrow 12.4 keV resonance of ^{45}Sc for future applications in extreme metrology [4].

Employing the 14.4 keV nuclear resonance of ^{57}Fe we aimed at the realization of multiphoton excitation in forward scattering from an ensemble of Mössbauer nuclei. Due to the radiative coupling between the nuclei in the ensemble, an enhanced decay rate (superradiance, SR) and collective energy shifts (collective Lamb shift, CLS) appear as characteristic signatures in the scattered light. So far, SR and CLS have been extensively studied in the single-photon excitation regime at synchrotrons. Here we wanted to address the spectral properties of the nuclear exciton under multiphoton excitation conditions, especially with the goal to determine the CLS as function of the number of photons that resonantly excite the nuclear ensemble. So far, the spectral properties under multiphoton excitation conditions have neither been approached theoretically nor experimentally.

The 12.4 keV resonance of ^{45}Sc is one of the narrowest nuclear resonances known with a half width of 1.4 femto-eV. In several aspects this isotope is superior to the 8.3 eV ^{229m}Th isomer for extreme metrology applications. The scientific potential of the ^{45}Sc resonance together with the possibility to resonantly excite it by photons from modern accelerator-based hard x-ray sources was identified more than 30 years ago [5]. However, it escaped detection until now, mostly due to the lack of hard x-ray sources with sufficient spectral flux. In this experiment the nuclear resonance of ^{45}Sc was successfully observed by irradiation of a Sc metal foil with 12.4-keV x-ray pulses of sub-millisecond duration and detection of the 4 keV delayed K-fluorescence that followed internal nuclear conversion. The resonance energy, which was known before the experiment to an uncertainty of +/- 50 eV only was determined with sub-eV accuracy. Our results set the stage for further studies of this isotope with promising applications in fundamental physics and extreme metrology.

Both experiments greatly benefitted from the high pulse repetition rate in conjunction with hard x-ray self-seeding (HXRSS) at the respective nuclear resonance energies, providing the spectral flux for efficient nuclear resonance excitation. A unique pulse pattern will be extremely beneficial for future studies at the ^{45}Sc resonance, in particular for the analysis of hyperfine interactions via nuclear forward scattering.

References

* Multiphoton Collective Lamb Shift
[1] E. Gerdau et al., *Nuclear Bragg diffraction of synchrotron radiation in yttrium iron garnet*, Phys. Rev. Lett. 54, 835 (1985)
[2] A. I. Chumakov et al., *Superradiance of an ensemble of nuclei excited by a free electron laser*, Nature Physics 14, 261 (2018)
[3] Experimental report #2778, *Multiphoton Collective Lambshift in Nuclear Resonant Scattering*
[4] Experimental report #3159, *Detection of the Ultranarrow Nuclear Resonance of 45-Sc*
[5] Yu. V. Shvyd'ko and G. V. Smirnov, *On the direct measurement of nuclear resonance parameters of long-lived (>~ 1 s) isomers*. Nucl. Instrum. Methods Phys. Res. B 51, 452 (1990)

Distinguishing Molecular Isomers by XFEL-based 3-D Coulomb Explosion Imaging

D. Rolles

J.R. Macdonald Laboratory, Kansas State University, Manhattan, KS, USA

After the successful proof of the XFEL-based Coulomb Explosion Imaging (X-CEI) method to image the molecular structure of ring molecules with 10+ atoms [1], we have extended the X-CEI method towards our ultimate goal of imaging *transient* molecular structures during ultrafast photochemical reactions. As a first step, we recorded static X-CEI patterns for three C_7H_8 isomers toluene (benzene ring with one methyl ligand), cycloheptatriene (7-member ring), and 1,6-heptadiyne (chain) to investigate how the different geometries are reflected in the X-CEI patterns, and to benchmark the predictions of our Coulomb explosion simulations. Next, we performed a time-resolved X-CEI experiment to track the UV-induced ring opening of the heterocyclic thiophenone (C_4H_4OS) molecule. The preliminary results of the time-resolved experiment, which took place in the REMI end-station at the SQS instrument at European XFEL approximately three months ago, demonstrate the impressive ability of the X-CEI method to image the full *three-dimensional* molecular geometry, including the position of hydrogen atoms, which are difficult to resolve via ultrafast diffraction techniques. Furthermore, although the analysis of the data capturing the initial phase of the ring-opening in the first 100 fs is still in progress, structural changes on the picosecond scale are clearly observed in the experimental data.

References

[1] R. Boll *et al.*, Nat. Phys. **18**, 423-428 (2022)

Mixing laser- and x-ray-beams for probing the electronic structure of solids by non-linear spectroscopy

Daniel Schick, MBI Berlin

Abstract

Free-electron laser sources are shifting the limits for non-linear spectroscopy into the extreme ultraviolet (XUV) and X-ray spectral ranges, where inner shell electrons become involved in the non-linear processes. Exemplarily, we studied the influence of core excitons in a lithium fluoride single crystal on sum- and difference-frequency mixing by employing XUV free-electron and optical laser pulses. This allows probing charge localization with atomic specificity and gives access to otherwise forbidden, dark transitions.

Distinguishing Molecular Isomers by XFEL-based 3-D Coulomb Explosion Imaging

D. Rolles

J.R. Macdonald Laboratory, Kansas State University, Manhattan, KS, USA

After the successful proof of the XFEL-based Coulomb Explosion Imaging (X-CEI) method to image the molecular structure of ring molecules with 10+ atoms [1], we have extended the X-CEI method towards our ultimate goal of imaging *transient* molecular structures during ultrafast photochemical reactions. As a first step, we recorded static X-CEI patterns for three C_7H_8 isomers toluene (benzene ring with one methyl ligand), cycloheptatriene (7-member ring), and 1,6-heptadiyne (chain) to investigate how the different geometries are reflected in the X-CEI patterns, and to benchmark the predictions of our Coulomb explosion simulations. Next, we performed a time-resolved X-CEI experiment to track the UV-induced ring opening of the heterocyclic thiophenone (C_4H_4OS) molecule. The preliminary results of the time-resolved experiment, which took place in the REMI end-station at the SQS instrument at European XFEL approximately three months ago, demonstrate the impressive ability of the X-CEI method to image the full *three-dimensional* molecular geometry, including the position of hydrogen atoms, which are difficult to resolve via ultrafast diffraction techniques. Furthermore, although the analysis of the data capturing the initial phase of the ring-opening in the first 100 fs is still in progress, structural changes on the picosecond scale are clearly observed in the experimental data.

References

[1] R. Boll *et al.*, Nat. Phys. **18**, 423-428 (2022)

Exploring fundamental electron dynamics with attosecond X-ray pulses

Markus Illchen, DESY

Abstract

Fundamental electron dynamics at the attosecond frontier and their direct coupling to structural dynamics of matter yield novel insights into the energy-distribution and protection mechanisms of Nature. The angular-streaking technique has exclusively demonstrated its capability of obtaining the full time-energy structure of XFEL pulses with attosecond resolution directly in the time-domain, thus enabling XFELs to study electron dynamics from element-specific vistas and their importance as onset of subsequent structural dynamics. Latest advances of this technique together with first results from the 2022 EuXFEL atto-campaign and the complementary prospects of the FLASH 2020+ innovation project at DESY will be presented.

The ultrafast interfacial movie-imaging electronic and structural dynamics at the space-time limit

Kiana Baumgärtner, U Würzburg

Abstract

Function is dynamic and arises at hybrid interfaces. In molecular devices such as mechanical switches or catalytic surfaces device function is often initiated by the transfer of charge and energy across the substrate-molecule interface and involves the interplay between electronic and structural degrees of freedom. By shooting a 'molecular movie' we aim to visualize and disentangle these electronic and structural dynamics with femtosecond temporal resolution and sub-Angström spatial resolution. For shooting the molecular movie we combine three modalities of time-resolved photoelectron spectroscopy (tr-ARPES, tr-XPS and tr-XPD) in one setup to simultaneously trace the sample's valence band and core level evolution with a time-of-flight momentum microscope. From the obtained four-dimensional datasets of energy, momentum-space and time we can trace the signatures of excited molecular states in time and decipher their role in initiating a macroscopic structural reorganization of the molecular film. We believe that our findings improve our understanding of intertwined electronic and structural processes at hybrid interfaces and will therefore enable the design of new functionalities in active hybrid matter.

Controlling x-ray matter interaction by collision-induced changes of electronic populations

A. Benediktovitch[1], L. Mercadier[2], D. Ronchetti[1], S. Bajt[1], S. Serkez[2], J.-E. Rubensson[3], B. Ziaja[1,4], SCS team[2], et al, N. Rohringer[1,5]
1) CFEL, DESY, Hamburg, Germany
2) European XFEL, Schenefeld, Germany
3) Uppsala University, Uppsala, Sweden
4) Institute of Nuclear Physics, Polish Academy of Sciences, Krakow, Poland
5) Universität Hamburg, Hamburg, Germany

The irradiation of a solid with focused soft x-ray FEL pulses transforms its constituent atoms into an electronically highly excited, transient state on an ultrashort time scale. In this regime, the solid is brought into the warm dense matter state and new bound-bound electron transitions may open – thus dramatically modifying the absorption as well as scattering properties of the solid. We present results of two recent experiments at the European XFEL SCS instrument that demonstrate these phenomena on copper.

In the first experiment, the XFEL pulse with a photon energy around the Cu L-edge is focused on a thin Cu foil, transforming Cu quasi instantaneously into an electronically excited state: L-shell photoionization and subsequent Auger-decay creates an out-of-equilibrium population of continuum electronic states. Electron-electron and electron-ion/atom collisions then drive the system to a state of warm dense matter on a 10-100 fs timescale. We probe this transient state by spectrally resolving the transmitted x-ray pulse as a function of fluence, thereby revealing the atomic and ionic properties. For XFEL pulse intensities above 10^{13} W/cm^2, we observe that a strong pre L-edge peak appears in the absorption spectrum which is due to $2p_{3/2} \rightarrow 3d$ transitions. These absorption channels open due to holes in the Cu 3d shell that are produced by electron-impact ionization. At higher fluence, the pre-edge peak broadens, drops, and the spectral absorption profile becomes smooth without a pronounced L–absorption edge. These features are consistent with the appearance of multiple higher ionic charge states in different electronic configurations, as our modeling based on the kinetic Boltzmann approach demonstrates.

In the second experiment, the x-ray scattering properties of the transient state are studied, by spectrally resolving the diffracted x-ray radiation with the hRIXS spectrometer: We investigated the diffracted spectral intensity of the 5th order superlattice peak of a $[B_4C(2nm)/Cu(2nm)/SiC(2nm)]_{15}$ multilayer sample. As expected from the fundamental relation between scattering and absorption, the opening of absorption channels on $2p_{3/2} \rightarrow 3d$ transitions likewise results in additional resonant elastic scattering contributions. In line with our first experiment, at XFEL intensities above 10^{13} W/cm^2 we observe a strong enhancement of the diffracted intensity in the pre-edge spectral region. This demonstration paves the way towards control of atomic scattering properties.

In the hard x-ray regime, we envision that the enhancement of atomic scattering factors, which also changes the phase of the scattering factor, becomes beneficial for structural crystallography. Thanks to enhanced scattering by transient resonant channels, the corresponding atoms would scatter like much heavier atoms – it could be beneficial for methods such as single-wavelength anomalous dispersion. This could pave the way to novel methods to solve the phase problem of x-ray scattering experiments.

Manipulation of host cells by infecting bacteria

Prof. Dr. Aymelt Itzen[1,2]

[1] University Medical Center Hamburg-Eppendorf (UKE), Center for Experimental Medicine, Institute of Biochemistry and Signaltransduction, Martinistr. 52, 20246 Hamburg

[2] Centre of Structural Systems Biology, University Medical Center Hamburg-Eppendorf (UKE)

Abstract

Bacterial pathogens are a global problem for our healthcare systems. Resistance to medically important antibiotics is increasing, leading to the spread of serious bacterial infections. This development poses increasing problems for hospitals and their patients. In particular, patients with a weakened immune system and the elderly are vulnerable to dangerous bacterial diseases.

Therefore, researchers are aiming to understand the molecular mechanisms of bacterial infections to potentially explore new treatment strategies in the long term. To this end, it is beneficial to understand in detail the interaction of bacteria with their human hosts and to study the infectiological characteristics of individual pathogens.

An interesting class of pathogens are bacteria that invade a human cell and multiply in this environment. These include, for example, Legionella, which can cause the infamous Legionnaires' disease. Legionella can be absorbed by humans into the lungs through contaminated aerosols. Once in the lungs, the bacteria attack immune cells and create a microenvironment within them in which they can survive and multiply. To this purpose, Legionella releases bacterial proteins via a syringe-like transport system that specifically manipulates the human host cell to meet the pathogen's demands. This battle zone of human and bacterial proteins represents an interesting field of research that offers the possibility to better understand the molecular strategies of infection processes.

My research group is therefore dedicated to the characterization of such bacterial proteins (e.g. Legionella proteins) and their interactions with human factors. Therefore, we study their interactions in atomic detail to understand the fundamentals of bacterial-human interactions. We obtain protein samples by biochemical and chemical-biological methods and subsequently perform structural biological studies. For this purpose, proteins are grown into crystals, which are then analyzed using brilliant synchrotron radiation. From the diffraction pattern and their intensities, conclusions can be drawn about the atomic composition and arrangement of proteins, providing valuable insights into the mechanisms of their activity. In my talk, I will show how the combination of biochemistry and structural biology can provide valuable new information on details of infection processes.

The state of zinc in methanol synthesis over a Zn/ZnO/Cu(211) model catalyst

Peter Amann[1,2], Bernhard Klötzer[3], David Degerman[1], Norbert Köpfle[3], Thomas Götsch[4], Patrick Lömker[1,6], Christoph Rameshan[5], Kevin Ploner[3], Djuro Bikaljevic[3], Hsin-Yi Wang[1], Markus Soldemo[1], Mikhail Shipilin[1], Christopher Goodwin[1], Jörgen Gladh[1], Joakim Stenlid[1], Mia Börner[1], Christoph Schlueter[6] and Anders Nilsson[1]

[1] *Department of Physics, Stockholm University, Sweden*

[2] *Present address: Scienta Omicron, Taunusstein, Germany*

[3] *Institute of Physical Chemistry, University of Innsbruck, Austria*

[4] *Fritz Haber Institute of the Max Planck Society, Berlin, Germany*

[5] *Institute of Materials Chemistry, Technical University Vienna, Vienna, Austria*

[6] *Deutsches Elektronen Synchrotron DESY, Hamburg, Germany*

Abstract

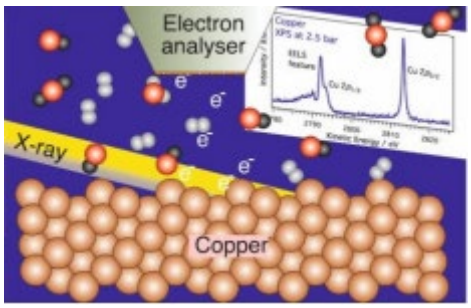

Methanol is a highly attractive base chemical that can give an important contribution for closing the carbon cycle when formed from a mixture of CO, CO2 and H2. While the elements Cu and ZnO show very low turnover rates, the mixture of them results in highly active catalysts. Despite intense investigations there have been significant unresolved questions on the nature of Zn: whether it is in a metallic or (partly)oxidized state or if Zn forms an alloy with Cu during the reaction.

Here I report on an experimental approach that allows investigation of the Zn state under operando conditions using a pressure greater than 180 mbar and variable temperature. The figure gives an artist's impression of the situation where a copper catalyst is surrounded by gas molecules and the reaction intermediates are probed with x-rays. We find that Zn dynamically responds to the chemical potential of the surrounding gas and becomes more metallic under CO hydrogenation conditions and more oxidized under CO2 hydrogenation conditions. By comparing with brass and polycrystalline Zn sample we can distinguish the different states of Zn as Zn metal islands, ZnO and surface Cu-Zn alloy. Under all conditions we find that Zn is in a mixed oxide- intermetallic state. The mixture of CO, CO2 and H2 critically affects the local ZnO ⇆ Zn redox equilibrium and we conclude that the most active phase is stabilized in the simultaneous presence of balanced amounts of CO, CO2 and H2. The results were achieved using the POLARIS instrument (Scienta Omicron, BarXPS) [Amann et al. RSI, 103102, 2019], at beamline P22 of the Petra III synchrotron at DESY, Germany. This instrument was designed at Stockholm University and allows for investigating catalysts under operando conditions at pressures of up to- and beyond 1 bar in combination with elevated temperature capabilities. Using grazing-incidence, hard X-rays from the synchrotron, the experiment can be optimized to a specific aspect with respect to bulk or surface sensitivity. This is done by stepping through the critical angle of total external reflection. The results got published in Science [Amann et al. Science 376, 2022]

Use of AI for synchrotron data analysis

Tobias Strohmann[1], Katrin Bugelnig[1], Joachim Gussone[1], Pere Barriobero-Vila[1,2], David Melching[1], Felix Bode[1], Eric Breitbarth[1], Andreas Stark[3], Norbert Schell[3], Fabian Wilde[3], Christoph Wielenberg[4], Julie Villanova[5], Elodie Boller[5], Guillermo Requena[1,6]

[1] *German Aerospace Center (DLR)*

[2] *Technical University of Catalonia (UPC)*

[3] *Helmholtz-Zentrum Hereon*

[4] *Premium Aerotec (PAG)*

[5] *European Synchrotron Radiation Facility (ESRF)*

[6] *RWTH Aachen University*

Abstract

The continuously increasing brilliance of synchrotron sources as well as the use of fast imaging detectors gives researchers access to a large amount of two-, three- or four-dimensional data. For materials scientists, such data contains information relevant to elucidate the relationships between process, microstructure and performance of materials.

Usually, the process of data preparation, e.g. the segmentation of tomography data, requires intensive and time-consuming manual work to be performed representing a bottleneck in the research process. Moreover, in many cases it is only possible to analyze synchrotron data once the researchers return from the synchrotron source back to their home labs. As a consequence, experiments have to be fully scheduled in advance to the beamtime. However, for many cases, a more *agile* experimental planning would be beneficial, i.e. fine-tuning of initial experimental parameters based on preliminary results of just accomplished experiments.

To enable such agile planning, we explored the usability of different approaches of deep learning algorithms and, particularly, convolutional neural networks (CNNs). CNNs present one state-of-the-art technique for pattern recognition in digital images of various domains. However, their application needs to be adapted to the specific needs of every field.

In this talk, we present results using deep learning for three materials science use cases:
Firstly, we explored the use of *unsupervised machine learning* to obtain fast insights into time-resolved high energy synchrotron diffraction obtained during in situ heat treatments of a Ti-6Al-4V alloy produced by additive manufacturing. To this purpose, we trained an autoencoder CNN model. The learned latent space representing diffraction pattern for individual time steps correlates well with the phase fraction of α/α' and β.
Secondly, a CNN was trained using *supervised machine learning* to segment the microstructural components of an AlSi cast alloy imaged using synchrotron X-ray tomography. The results show that this approach can reduce the total working time for the segmentation tremendously compared to a manual segmentation. Lastly, we give an outlook on the use of *generative neural networks* to increase the spatial resolution of synchrotron X-ray computed tomography.

POSTER LIST

Poster Session Topics

Wednesday Jan 25, 2023: Posters 1 to 161

Thursday Jan 26, 2023: Posters 162 to 342

III.1 European XFEL

1. The Femtosecond X-ray Experiments (FXE) Instrument at the European XFEL: current status and recent results
   Y. Jiang, F. Alves Lima, F. Ardana-Lamas, M. Biednov, D. Bregenholt Jakobsen, P. Frankenberger, X. Huang, D. Khakhulin, M. Knoll, S. Paul Dutta, V. Tiwari, Y. Uemura, H. Wang, H. Yousef, P. Zalden and C. Milne

2. Pump–probe capabilities at SPB/SFX, European XFEL
   J. Koliyadu, R. Letrun, J. Liu, M. Jiang, M. Emons, T. Dietze, N. Reimers, R. Bean and T. Sato

3. Tracking the origin of the MnAs magneto-structural phase transitions in the time-domain using femtosecond X-ray diffraction
   F. Vidal, Y. Zheng, E. Ferrari, M. Eddrief, P. Atkinson, N. Casaretto, L. Lounis, L. Coelho, C. Laulh'e, H. Popescu, C. Spezzani, E. Allaria, A. Ciavardini, H. Wang, J. Ma, J. Zhao, M. Seaberg, R. Alonso-Mori, J. Glownia, M. Chollet, D. Khakhulin, F. Ardana Lamas, Y. Uemura, M. Biednov, F. A. Lima, P. Zalden, C. Milne and M. Sacchi

4. High Energy X-ray Emission spectrometer with Laue analyzer
   X. Huang, F. Lima and C. Milne

5. Numerical Simulation of SFX Sample Delivery Systems
   B. Šarler, S. Bajt, H. Chapman, B. Mavrič, K. Kovačič, K. Bakhat Rana, Z. Rek, G. Savšek, R. Zahoor and B. Zupan

6. Atomic structure of recombinant high potential iron sulfur protein in its reduced and oxidized states revealed by serial femtosecond crystallography
   F.H.M. Koua, J. Bielecki, M. Kloos, P. Vagovic, H. Han, J. Schulz and A. Mancuso

7. Mix-and-Inject Sample Delivery Systems for Time-resolved Serial Crystallography
   M. Vakili

8. Rapid structural transformations in Fe after sub-ps pulsed laser annealing
   R. Sobierajski, P. Zalden, K. Sokolowski-Tinten, A. Olczak, C. Bressler, M. Chojnacki, P. Dluzewski, P. Dziegielewski, A.R. Fernandez, K. Fronc, W. Gawelda, K. Georgarakis, A.L. Greer, J. Hastings, I. Jacyna, R. Kaminski, R.W.E. van de Kruijs, D. Khakhulin, D. Klinger, K. Kosyl, K. Kubicek, I. Milov, O. Liubchenko, K. Morawiec, N. Panagiotopoulos, M. Sikora, P. Sun, H. Yousef and J. Antonowicz

9. Two-dimensional energy and carrier diffusion in silicon upon X-ray irradiation
   V. Lipp and B. Ziaja

10. MS SPIDOC: Coherent Diffractive Imaging of proteins and viral capsids
    T. Kierspel, A. Kádek, J.C.K. Kung, T. Damjanović and C. Uetrecht

11. Ultrafast melting of optically excited thin polycrystalline palladium films
    J. Antonowicz, P. Zalden, K. Sokolowski-Tinten, A. Olczak, I. Milov, C. Bressler, M. Chojnacki, P. Dziegielewski, G. Evangelakis, A.R. Fernandez, K. Fronc, W. Gawelda, K. Georgarakis, A.L. Greer, I. Jacyna, R.W.E. van de Kruijsi, R. Kaminski, D. Khakhulin, D. Klinger, K. Kosyl, K. Kubicek, N. Panagiotopoulos, M. Sikora, P. Sun, H. Yousef and R. Sobierajski

12. X-ray diffractive imaging of UV-induced ultrafast dynamics in CF_2I_2
    N. Vadassery, S. Trippel and J. Küpper

13. Reference-enhanced Single Particle Imaging
A. Mall and K. Ayyer

14. A brief overview of FEA/CFD simulations at European XFEL
F. Yang and D. La Civita

15. Hardware Acceleration for Data Processing at Synchrotrons and FELs
S.P. Ramakantha Setty, V. Rahmani, S. Nawaz, D. Pennicard and H. Graafsma

16. Cu Kα, K$\beta_{1,3}$, and K$\beta_{2,5}$ X-ray Emission Spectroscopic Study of Photoexcited [Cu(dmp)$_2$]$^+$ at FXE Instrument
T.-K. Choi, D. Khakhulin, F. A. Lima, M. Biednov, Y. Uemura, A. Burgos, A. Glinka, J. F. Hidalgo, R. T. Ramirez, Z. Németh, J. Szlachetko, S. Nozawa, S. Adachi, T. Penfold, C. Milne, G. Vankó, W. Gawelda and T. Katayama

17. Towards Serial Femtosecond X-ray Photocrystallography of Molecular Materials at FXE instrument.
D. Vinci, Y. Jang, M. Lorenc, C. Mariette, R. van der Veen, H. Mueller-Werkmeister, R. J. Kaminski, K. N. Jarzembska, R. Schubert, K. Ridier, P. Zelden, F. Ardana Lamas and C. Deiter

18. Structural dynamics of shock-compressed water - Combined WAXS and Near-Field Holography at EuXFEL
H.P. Hoeppe, M. Vassholz, J. Hagemann, J. M. Rosselló, M. Osterhoff, R. Mettin, J. Möller, M. Scholz, U. Boesenberg, J. Hallmann, C. Kim, A. Zozulya, W. Lu, R. Shayduk, A. Madsen and T. Salditt

19. Pump-probe serial crystallography on perovskite quantum dots
Z. Shen and K. Ayyer

20. Conformation space sampling based on Monte Carlo method in XFEL experiment
Z. Shen, K. Ayyer and D. Loh

21. Data Reduction for X-ray Serial Crystallography using Machine Learning
V. Rahmani, S. Nawaz, S. Pala Setty, D. Pennicard and H. Graafsma

22. Deep learning image reconstruction approaches towards MHz X-ray microscopy
Y. Zhang, Z. Yao, M.A. Noack, P. Vagovic, K. Fezzaa, F. Garcia-Moreno, T. Ritschel and P. Villanueva-Perez

23. Performance analysis of x-ray Optical Delay Line at European XFEL
M. Tavakkoly, J. Gruenert, A. Koch, D. La Civita, M. Makita, M. Meyer, M. Planas, S. Serkez, H. Sinn, T. Wohlenberg and M. Vannoni

24. First high energy and temporal resolution pump probe RIXS at the EuXFEL
L. Adriano, A. Alic, D.R. Baykusheva, R. Carley, G.S. Chiuzbaian, M.P.M. Dean, O. Duros, A. Foelisch, M. Foerst, B.K. Freelon, N. Gerasimova, G. Ghiringhelli, X. Jiang, D. Jost, M. Kusch, T. Laarman, V. Lebedev, W.S. Lee, C.Y. Liu, L. Martinelli, L. Mercadier, G.Merzoni, M.Minola, M. Mitrano, S. Molodtsov, C.S. Pathiraja, S. Parchenko, J.N. Ranhili Pelige, Y. Peng, Q. Qiu, T. Schmitt, J. Sears, A. Scherz, S. Sreenkatan Nair Lalithambika, S. Techert, M. Teichmann, S.F.R. TenHuisen, B. van Kuiken, Z. Yin and J. Schlappa.

25. Structural dynamics of ferroelectric thin films
L. P. Hoang, I. Spasojevic, R. Carley, L. Mercadier, M. Teichmann, D. Hickin, N. Domingo, G. Catalan, J. Zegenhagen, K. Rossnagel, I.A. Vartanyants, T.-L. Lee, A. Scherz and G. Mercurio.

26. Using fast jets as liquid sample delivery for femtosecond pump-probe experiments at the FXE instrument: A blessing and a curse of the MHz rates
H. Wang, F. Lima, M. Vakili, C. Milne, F. Otte, P. Zalden, P. Frankenberger, M. Knoll, Y. Uemura, F. Ardana Llamas, M. Biednov, Y. Jiang, D. Khakhulin, S. Haryati Binti, M. Heder, D. Vinci, D. Bregenholt Jakobsen, S. P. Dutta and X. Huang

27. Probing broadband multi-THz coherent phonons in SrTiO3 and Si on a crystal truncation rod with femtosecond X-ray diffraction
R. Shayduk, J. Hallmann, A. Rodriguez-Fernandez, M. Scholz, W. Lu, U. Bösenberg, J. Möller, A. Zozulya, M. Jiang, U. Wegner, R.-C. Secareanu, G. Palmer, M. Emons, M. Lederer, S. Volkov, I. Lindfors-Vrejoiu, D. Schick, M. Herzog, M. Bargheer, J.-E. Pudell and A. Madsen

28. Probing protein diffusion with X-ray Photon Correlation Spectroscopy at European XFEL
A. Girelli, M. Filianina, M. Bin, S. Berkowicz, N. Das Anthuparambil, M. Paulus, S. Timmermann, M. Akhundzadeh Sayed, M. Senft, S. Retzbach, M. Dargasz, M. Kowalski, Y. Chushkin, N. Begam, M. Reiser, A. Ragulskaya, A. Zozulya, T. Seydel, A. Madsen, J. Moeller, J. Hallmann, A. Rodriguez-Fernandez, F. Schreiber, F. Zhang, C. Gutt and F. Perakis

29. Modelling of ultrafast X-ray induced magnetization dynamics in magnetic systems
K. Kapcia, V. Tkachenko, F. Capotondi, A. Lichtenstein, S. Molodtsov, L. Mueller, A. Philippi-Kobs, P. Piekarz and B. Ziaja

30. THz SASE FEL at PITZ as a prototype of a tunable THz source for pump-probe experiments at the European XFEL
M. Krasilnikov, Z. Aboulbanine, G. Adhikari, N. Aftab, A. Asoyan, P. Boonpornprasert, H. Davtyan, D. Dmytriiev, G. Georgiev, J. Good, A. Grebinyk, M. Gross, A. Hoffmann, X.-K. Li, A. Lueangaramwong, D. Melkumyan, S. Mohanty, R. Niemczyk, A. Oppelt, H. Qian, C. Richard, F. Stephan, G. Vashchenko, T. Weilbach, E. Schneidmiller, M. Yurkov, W. Hillert and J. Rossbach

31. Programmable DNA-Origami Molecular Scaffolds for Holographic Single-Particle Diffractive Imaging with XFEL Pulses
P.L. Xavier, N.C. Seeman and H.N. Chapman

32. Phase transition kinetics and surface morphology in femtosecond laser-heated metals
Ö. Öztürk, M. Nakatsutsumi, J.P. Schwinkendorf, Z. Chen, B. Rethfeld, V. Recoules, L. Randolph, C. Gutt, C. Roedel, T. Kluge, L. Huang, T.R. Preston, M. Makita, S. Goede, E. Brambrink, A. Pelka, M. Banjafar, S.V. Rahul, L.P. Wollenweber, H. Hoeppner, C. Baehtz, S.H. Glenzer, G. Jakob, B. Cho, M. Mo, P.T. Terekhin, F. Brieuc, M. Klaeui and B. Schwendeman

33. The unique sensitivity of Cr Kα_1 emission line reveals early excited state landscape of the molecular ruby
M. Nowakowski, W. Kitzmann, M. Biednov, D. Khakhulin, F. Alves Lima, C. Milne, L. Stein, L. Fritsch, F. Reichenauer, F. Otte, K. Heinze and M. Bauer

34. Online dynamic flat-field correction for MHz XFEL microscopy
S. Birnsteinova, D.E. Ferreira de Lima, E. Sobolev, V. Bellucci, C. Kim, T. Sato, R. Bean, G. Giovanetti, K. Buakor, Y. Zhang, A.P. Mancuso, P. Villanueva-Perez and P. Vagovič

35. Multiple-core-hole resonance spectroscopy with ultraintense x-ray pulses
A. Rörig, S.-K. Son, T. Mazza, P. Schmidt, T.M. Baumann, B. Erk, M. Ilchen, J. Laksman, V. Music, S. Pathak, D.E. Rivas, D. Rolles, S. Serkez, S. Usenko, R. Santra, M. Meyer and R. Boll

36. Ultrafast X-Ray Pump X-Ray Probe Absorption Spectroscopy of Warm Dense Copper
L. Mercadier, A. Benediktovitch, S. Krušič, M. Agåker, R. Carley, G. Fazio, N. Gerasimova, Y. Y. Kim, L. Le Guyader, G. Mercurio, S. Parchenko, J.-E. Rubensson, J. Schlappa, S. Serkez, M. Stransky, M. Teichmann, Z. Yin, M. Žitnik, A. Scherz, B. Ziaja and N. Rohringer

37. Photon shot-noise limited transient absorption soft X-ray spectroscopy at the European XFEL
L. Le Guyader, A. Eschenlohr, M. Beye, W. Schlotter, F. Döring, C. Carinan, D. Hickin, N. Agarwal, Ch. Boeglin, U. Bovensiepen, J. Buck, R. Carley, A. Castoldi, A. D'Elia, J. T. Delitz, W. Ehsan, R. Engel, F. Erdinger, H. Fangohr, P. Fischer, C. Fiorini, A. Föhlisch, L. Gelisio, M. Gensch, N. Gerasimova, R. Gort, K. Hansen, S. Hauf, M. Izquierdo, E. Jal, E. Kamil, S. Karabekyan, T. Kluyver, T. Laarmann, T. Lojewski, D. Lomidze, S. Maffessanti, T. Mamyrbayev, A. Marcelli, L. Mercadier, G. Mercurio, P.S. Miedema, K. Ollefs, K. Rossnagel, B. Rösner, N. Rothenbach, A. Samartsev, J. Schlappa, K. Setoodehnia, G. Sorin Chiuzbaian, L. Spieker, Ch. Stamm, F. Stellato, S. Techert, M. Teichmann,

M. Turcato, B. Van Kuiken, H. Wende, A. Yaroslavtsev, J. Zhu, S. Molodtsov, Ch. David, M. Porro and A. Scherz

38. Selection and control of (bio-)nanoparticles with external fields
X. Cheng, L. V. Haas, J. Lübke, M. Amin, A.K. Samanta and J. Küpper

39. A diamond channel cut monochromator for intense MHz repetition rate operation at EuXFEL: first experimental results
K.R. Tasca, U. Bösenberg, F. Brausse, A. Madsen, J. Möller, I. Petrov, A. Rodriguez-Fernandez, R. Shayduk, H. Sinn, M. Vannoni, J. Wonhyuk, M. Youssef, P. Zalden, A. Zozulya and L. Samoylova

40. Single-particle Diffractive Imaging at the European XFEL: Instrumentation, Data Acquisition and Hit-finding
M. Stammer, C. Neuhaus, J. Alfken, M. Osterhoff, R. Bean, J. Bielecki, J. E, S. Rafie-Zinedine, R. de Wijn, R. Letrun, A. Mancuso, R. Jahn and T. Salditt

41. Scientific Data Management at European XFEL.
N. Alqudami, S. Aplin, D. Boukhelef, F. Dall'Antonia, I. Derevianko, U. Ensslin, M. Gasthuber, J. Hannappel, M. Karimi, T. Kluyver, L. Maia, J. Malka, M. Manetti, T. Mkrtchyan, K. Ohrenberg, C. Patzke, G. Previtali, P. Schmidt, K. Schwarz, E. Sobolev, J. Szuba, B. Vanganuru, C. Voss, K. Wrona and C. Youngman

42. Alpha-synuclein fiber diffraction at EuXFEL
M. Beltramini, L. Bubacco, M.G. Ortore, P. Mariani, S. Morante, N. Plotegher, M. Polentarutti, M. Sandre, F. Spinozzi, F. Stellato and I. Tessari

43. Spectral metrology for MHz multi-projection X-ray microscopy
I. Petrov, V. Bellucci, S. Birnsteinova, L. Samoylova and P. Vagovic

44. 3D structure determination via correlated x-ray scattering from disordered ensembles of particles
T.B. Berberich, S.L. Molodtsov, A. I. Lichtenstein and R.P. Kurta

45. Update status of beam conditioning optics and options for harder X-rays above 30 keV at the MID instrument of EuXFEL
A. Zozulya, G. Ansaldi, U. Bösenberg, F. Braußе, J. Hallmann, W. Jo, W. Lu, J. Möller, J. Pudell, A. Rodriguez-Fernandez, R. Shayduk, K. Sukharnikov, M. Youssef, L. Batchelor, M. Dommach, L. Samoylova, H. Sinn, M. Vannoni and A. Madsen

46. Hydrogen Metallisation in Warm Dense Matter condition
D. Ranjan, K. Ramakrishna, J. Vorberger and D. Kraus

47. High repetition rate velocity map imaging using the Timepix3 camera at the SQS instrument
B. Senfftleben, R. Boll, A. Alangattuthodi, T. Baumann, V. Bondar, H. Bromberger, S. Dold, B. Erk, A. De Fanis, T. Jahnke, J. Küpper, T. Mazza, J. Montaño, T. Mullins, Y. Ovcharenko, A. Parenti, N. Rennhack, D. Rivas, A. Rörig, S. Sasikumar, P. Schmidt, M. Togawa, S. Trippel, S. Usenko, R. Wagner and M. Meyer

48. Investigation of protein dynamics in crowded environments at European XFEL with MHz XPCS
M. Dargasz, M. Reiser, A. Girelli, A. Ragulskaya, S. Das, S. Berkowicz, M. Bin, M. Ladd-Parada, M. Filianina, H. Poggemann, N. Begam, M. Sayed Akhundzadeh, S. Timmermann, L. Randolph, Y. Chushkin, T. Seydel, U. Boesenberg, J. Hallmann, J. Möller, A. Rodriguez-Fernandez, R. Rosca, R. Schaffer, M. Scholz, R. Shayduk, A. Zozulya, A. Madsen, F. Schreiber, F. Zhang, F. Perakis and C. Gutt

49. Supramolecular dynamics investigated on hydrogen bonded pyrrole/indole-water clusters upon site-specific x-ray photoionization
I.S. Vinklárek, D. Koulentianos, H. Bromberger, W. Jin, R. Boll, M. Meyer, S. Trippel and J. Küpper

50. Micro- and Nanofocus Characterization by Ablative Imprints at SQS and HED Instruments
Š. Jelínek, K. Appel, T. Baumann, E. Brambrink, T. Burian, S. Dold, J. Grünert, V. Hájková, L. Juha,

Z. Konopková, Z. Kuglerová, N. Kujala, H. Lee, S. Makarov, M. Makita, T. Mazza, M. Meyer, L. Mikeš, B. Nagler, M. Nakatsutsumi, Y. Ovcharenko, S. Pikuz, T. Pikuz, T. R. Preston, A. Schropp, S. Usenko, P. Vagovič, V. Vozda, U. Zastrau and J. Chalupský

51. The Heisenberg RIXS instrument at SCS, European XFEL - ultrafast spectroscopy at the limit of energy and time resolution
J. Schlappa, G. Ghiringhelli, B. Van Kuiken, M. Teichmann, P. Miedema, J. T. Delitz, N. Gerasimova, S. Molodtsov, L. Adriano, B. Baranasic, C. Broers, R. Carley, P. Gessler, N. Ghodrati, D. Hickin, L. P. Hoang, M. Izquierdo, G. Mercurio, S. Parchenko, M. Stupar, Z. Yin, L. Martinelli, G. Merzoni, Y. Peng, T. Reuss, S. Sreekantan Nair Lalithambika, S. Techert, T. Laarmann, S. Huotari, C. Schroeter, B. Langer, T. Giessel, S. Neppl, R. Buechner, J. Buchheim, V. Vaz da Cruz, S. Eckert, G. Gwalt, C.-Y. Liu, F. Siewert, C. Sohrt, C. Weniger, A. Pietzsch, F. Senf, A. Scherz and A. Fohlisch

52. Coulomb Explosion Imaging of Ring Opening in Thiophenone
K. Chen, S. Bhattacharyya, A. Venkatachalam, H. Lam, E. Wang, K. Borne, D. Rivas, T. Mullins, S. Usenko, B. Senfftleben, F. Allum, A. Green, R. Ingle, E. Warne, J. McManus, R. Forbes, R. Tanyag, K. Lin, T. Baumann, F. Trinter, B. Erk, L.M. Ibele, B.F.E. Curchod, M.N.R. Ashfold, M. Burt, M. Brouard, J.P.F. Nunes, M.Centurion, P. Weber, M. Meyer, T. Jahnke, R. Boll, A. Rudenko and D. Rolles

53. Towards probing K-shell ionization of carbon under warm dense matter
C. Qu, J. Lütgert, D. Ranjan, B. Heuser, M. G. Stevenson, S. Schumacher, P. T. May, O. S. Humphries, L. Huang, U. Zastrau and D. Kraus

54. Status of FAST-XPD: Photon data base for the European XFEL
M. Manetti, L. Samoylova, H. Sinn, J. Szuba, K. Wrona, M. Yurkov and I. Zagorodnov

55. Following laser-driven dynamics with atomic resolution and with attosecond x-ray pulses
D. Gorelova

56. Nonlinear generation of wavelength tunable sub-10fs DUV pulses at MHz repetition rates
A. Alangattuthodi, M. Emons, R. Fabbri, J. Meier, J. Montano, D. Rivas, R. Secareanu, U. Wegner, D. Rompotis, M. Lederer, T. Mullins and M. Meyer

57. Simulating X-ray scattering: from large crystals to single molecules
S. Cardoch, I. Dawod, C. Caleman, F. Maia and N. Timneanu

58. Sample Environment and Characterization support at the European XFEL
J. Schulz and the SEC team

59. Instrumentation development for Multi-Projection X-ray imaging at EuXFEL
V. Bellucci, S. Birnsteinova, T. Sato, R. Letrun, J. Koliyadu, C. Kim, G. Giovanetti, R. Graceffa, L. Adriano, A. Mazzolari, M. Romagnoni, H. Huelsen, T. Nhi Tran Calliste, D. Korytar, P. Villanueva-Perez, E. Myrto Asimakopoulou, Z. Yao, Y. Zhang Yuhe, J. Ulicny, L. Samoylova, I. Petrov, A. Meents, C. Deiter, L. Lopez Morillo, R. Bean, H.N. Chapman, A. Mancuso and P. Vagovic

60. MHz rate XFEL beam position measurements with a Diamond Sensor
W. Freund, T. Conka Yildiz, J. Liu and J. Grünert

61. Towards a new scientific data policy for European XFEL
F. Dall'Antonia, J. Malka, E. Sobolev, P. Schmidt, L. Gelisio and K. Wrona

62. In situ X-ray diffraction of α-ϵ phase transition in iron under dynamic diamond anvil cell compression at EuXFEL
M. Tang, R.J. Husband, Z. Konôpková and C. Strohm

63. Ultrafast Magnetization Dynamics of Nanoscale Domains in Ferrimagnetic DyCo Films with Perpendicular Magnetic Anisotropy Studied at European XFEL
S. Marotzke, A. Philippi-Kobs, M. Riepp, L. Müller, W. Rosecker, D. Lott, C. Min, C. Luo, K. Chen, R. Frömter, H.P. Oepen, R. Carley, G. Mercurio, L.P. Hoang, S. Parchenko, L.L. Guyader, K. Rossnagel, F. Radu, A. Scherz and G. Grübel

hivolt.de

»HIGH VOLTAGE
POWER SUPPLIES

»HIGH VOLTAGE AMPLIFIERS

»HIGH VOLTAGE
CABLE & CONNECTORS

»MAGNET POWER SUPPLIES

hivolt.de GmbH & Co. KG
Oehleckerring 40 · D-22419 Hamburg
Telefon: +49 40 537122-80 · Fax: +49 40 537122-99
E-Mail: info@hivolt.de · Internet: www.hivolt.de

hivolt.de

www.hivolt.de

Wir bieten
HOCHSPANNUNG

PFIFFIGE KÖPFE
Wir suchen

64. Investigating ultra-fast geminal recombination in aqueous octahedral metal-hexacyanides with the hRIXS instrument at SCS
V. Vaz da Cruz, S. Eckert, E. J. Mascarenhas, M. Fondell, A. Pietzsch, T. Laarman, R. Carley, L. Mercadier, T. C. Asmara, M. Teichmann, L. Adriano, Z. Yin, B. Van Kuiken and A. Föhlisch

65. The results of the satellite workshop “High Rep Rate Fixed Target Delivery: Chip standardisation and workflow”
C. Deiter, A. Kardoost, E. Round and J. Schulz

66. Future Laser-based Terahertz Light Sources at European XFEL
I. Radu, R. Ivanov, B. Monoszlai, J. Meier, D. Rompotis, R. Secareanu, M. Emons, R. Fabbri, D. Kane, U. Wegner and M. Lederer

67. Enhancing soft x-ray diffraction by collision-induced manipulation of electronic populations
D. Ronchetti, A. Benediktovitch, L. Mercadier, S. Bajt, O. N. Yefanov, H. Chapman and N. Rohringer

68. Towards the direct x-ray-excitation of the ultra-narrow nuclear resonance of ^{45}Sc
Y. Shvyd'ko, R. Röhlsberger, O. Kocharovskaya, J. Evers, G. A. Geloni, P. Liu, A. Miceli, D. Shu, B. Stone, I. Uschmann, R. Lötzsch, W. Hippler, O. Leupold, I. Sergeev, H.-C. Wille, X. Zhang, M. Gerharz, S. Liu, N. Kujala, C. Grech, T. Kolodziej, A. Madsen, A. Zozulya, J. Hallman, U. Bösenberg and M. Youssef

69. Online Characterization of X-ray Pulses at the Attosecond Frontier
L. Funke, K. Dingel, A. Held, S. Savio, L. Wülfing, N. Wieland, M. Ilchen and W. Helml

70. Coherent Diffractive Imaging of Lipid and Synaptic Vesicles by Femtosecond XFEL pulses
C. Neuhaus, J. Alfken, M. Stammer, K. Komorowski, A. Major, R. Bean, J. Bielecki, J. E, S. Rafie-Zinedine, R. de Wijn, R. Letrun, R. Jahn and T. Salditt

71. Determination of thermalized fraction of intense short-wavelength radiation absorbed in solids: from UV to x-ray lasers
Z. Kuglerova, J. Chalupsky, R. Dudzak, T. Burian, M. Makita, P. Vagovic and L. Juha

72. Efficient time-resolved Laue diffraction data analysis for small and medium-sized molecules using novel seed-skewness algorithm
P. Laski, D. Szarejko, R. Kaminski and K.N. Jarzembska

73. Numerical Simulation of SFX Sample Delivery Systems
B. Šarler, S. Bajt, H. Chapman, B. Mavrič, K. Kovačič, K. Bakhat Rana, Z. Rek, G. Savšek, R. Zahoor and B. Zupan

III.2 FLASH

74. How to increase the efficiency of differential pumping
M. Degenhardt, M. Braune, S. Aref, F. Jastrow, M. Brachmanski and K. Tiedtke

75. Site-selective probing of ultrafast non-adiabatic photochemistry in CS_2
F. Allum, I. Gabalski, J. Unwin, I. Seidu, M, Britton, M. Brouard, P.H. Bucksbaum, J. P. Cryan, N. Ekanayake, D. Garg, E. Gougoula, D. Heathcote, A.J. Howard, P. Hockett, D.M.P. Holland, C-S. Lam, J.W.L. Lee, J. McManus, J. Mikosch, D. Milesevic, R.S. Minns, S.P. Neville, C. Passow, C. Papadopolou, W.O. Razmus, A. Röder, D. Rolles, A. Rouzée, A. Rudenko, M. Schnell, A. Simao, A. Stolow, C. Vallance, T. Walmsley, J. Wang, B. Erk, M.B. Burt, M.S. Schuurman and R. Forbes

76. New insights into the laser-assisted photoelectric effect from solid state surfaces
L. Wenthaus, N. Kabachnik, M. Borgwardt, S. Palutke, D. Kutnyakhov, F. Pressacco, M. Scholz, D. Potorochin, N. Wind, S. Düsterer, G. Brenner, O. Gessner, S. Molodtsov, W. Eberhardt and F. Roth

77. Ultra-broadband miniature FTIR spectrometer for characterization of IR and THz sources
E. Zapolnova, E. Jung S.-G. Gang and R. Pan

78. Single-shot temporal characterization of XUV FEL@FLASH
M. Bidhendi, R. Ivanov, I. Bermudez, J. Rönsch-Schulenburg, M. Vogt, M. V. Yurkov and S. Düsterer

79. Femtosecond laser spectroscopy for Exploration of Space
N. Stojanovic, Y. Ha, J. Petrovic, M. Rabasovic, A.Krmpot and M. Gensch

80. Relaxation dynamics in Xenon dimers and trimers after XUV-photoionization at FLASH2
H. Lindenblatt, K. Schnorr, S. Augustin, S. Meister, F. Trost, P. Schoch, G. Schmid, Y. Liu, M. Braune, M. Kuhlmann, R. Treusch, C. Schröter, T. Pfeifer and R. Moshammer

81. Start to End Simulation Results for Seeded FEL from FLASH Beams
P. Niknejadi, D. Samoilenko, P. Amstutz, T. Lang, S. Ackermann, F. Pannek, G. Paraskaki, E. Ferrari, S. Schreiber and L. Schaper

82. Diagnostics and applications of THz radiation at FLASH1 after FLASH2020+
S. Gang, E. Zapolnova, M. Temme, E. Ploenjes and R. Pan

83. FLASH2020+: SLASH a novel high power seed laser for two-color EEHG XUV/VUV FEL seeding
T. Lang, M.M. Kazemi, J. Zheng, S. Hartwell, N. Hoang, E. Ferrari, E. Allaria, L. Schaper and I. Hartl

84. Ultrafast photoinduced dynamics at the interface of water and anatase TiO_2(101)
M. Wagstaffe, A. Dominguez-Castro, L. Wenthaus, S. Palutke, D. Kutnyakhov, M. Heber, F. Pressacco, S. Dziarzhytski, H. Gleissner, V. Kristin Gupta, H. Redlin, A. Dominguez, T. Frauenheim, A. Rubio, H. Noei and A. Stierle

85. Analysis of ablation imprints accelerated by machine learning
J. Chalupský, V. Vozda, J. Hering, J. Kybic, T. Burian, S. Dziarzhytski, V. Hájková, Š. Jelínek, L. Juha, K. Juráňová, B. Keitel, Z. Kuglerová, M. Kuhlmann, B. Petryshak, M. Ruiz-Lopez, L. Vyšín, T. Wodzinsk and E. Plönjes

86. ML methods for an improved evaluation of FEL diagnosic data
G. Goetzke, G. Hartmann, S. Düsterer, F. Möller and C. Behrens

87. Climbing the N-shell resonance ladder of xenon
S. Palutke, M. Martins, S. Klumpp, K. Baev, M. Richter, T. Wagner, M. Kuhlmann, M. Ruiz-Lopez, M. Meyer and K. Tiedtke

88. Double electron spectrometer setup for time-resolved photoelectron spectroscopy at FELs
L. Wenthaus, S. Paltuke, D. Kutnyakhov, H.D. Meyer, S. Gieschen and M. Martins

89. Direct observation of phonon-electron energy flow in laser-heated Nickel
V. Shokeen, X. Wang, A. Yaroslavtsev, D. Kutnyakhov, M. Heber, P. Maldonado, Peter M. Oppeneer, H.-J. Elmers, G. Schönhense, N. Wind, L. Wenthaus, F. Pressacco, Sanjoy K. Mahatha, K. Rossnagel and H.A. Dürr

90. Advanced Diagnostic Perspectives for FLASH 2020+
M. Ilchen, C. Behrens, I. Bermudez Macias, Y. Bican, M. Bidhendi, M. Braune, M. Degenhardt, S. Düsterer, G. Goetzke, R. Ivanov, F. Jastrow, V. Music, S. Palutke, C. Passow, S. Savio, W. Helml and K. Tiedtke

91. Investigation of the coherence properties of FEL radiation at FLASH2
R. Quenter, M. Dreimann, D. Eckermann, S. Roling, V. Kärcher, M. Wöstmann, T. Reiker, M. von Piechowski, P.G. Shine, F. Rosenthal, M. Kuhlmann, S. Toleikis, R. Treusch, E. Plönjes-Palm and H. Zacharias

92. Performance of the XUV and soft x-ray split-and-delay unit at FLASH2
M. Dreimann, F. Wahlert, D. Eckermann, F. Rosenthal, S. Roling, T. Reiker, M. Kuhlmann, S. Toleikis, M. Brachmanski, R. Treusch, E. Plönjes-Palm, B. Siemer and H. Zacharias

93. Ultrafast Photodynamics of N3 Dye on the Electron Collector TiO_2
J. Davies, Y. Zhang, H. Fielding and G. Thornton

94. Time–resolved energy–momentum microscopy using FEL and multispectral HHG radiation
N. Wind, M. Heber, D. Kutnyakhov, F. Pressacco and K. Rossnagel

95. A hard X-Ray Split-and-Delay Unit for the HED Instrument at the European XFEL
D. Eckermann, S. Roling, M. Rollnik, P. Gawlitza, K. Appel, L. Samoylova, H. Sinn, F. Siewert, T. Tschentscher, F. Wahlert and U. Zastrau und H. Zacharias

96. Time-resolved XPS study of charge carrier dynamics at the MnPc/C_{60} heterointerface
D. Potorochin, L. Wenthaus, S. Palutke, D. Kutnyakhov, F. Pressacco, M. Scholz, N. Wind, M. Fraund, G. Brenner, O. Gessner, S. Molodtsov, W. Eberhardt and F. Roth

III.3 Other/external/theory

97. Recent developments in nanostructured X-ray optics in three, two and 2.5 dimensions
A. Kubec, J. Erjawetz, C. David and F. Döring

98. snip – digital lab book from a users' perspective
M. Osterhoff, Sebastian Mohr and S. Köster

99. Dynamical diffraction echoes as streaking method to image ultrafast processes
A. Rodriguez-Fernandez

100. Helmholtz Imaging
P. Heuser, D. Schmidt, F. Isensee, K. Sander and S. Krause-Solberg

101. The DESY NanoLab
H. Noei, T.F. Keller, V. Vonk, R. Röhlsberger and A. Stierle

102. Structural insight into the binding mode of sisomicin derivatives and gentamicin C2b to the decoding center of the 30S ribosomal subunit
E. Destan and H. DeMirci

103. Aqueous Solvation of Iodide - Structural dynamics observed by time resolved X ray solution scattering
V. Markmann, J. Pan and K. Haldrup

104. Theoretical description of X-ray absorption by laser-driven electronic system
T. Bezriadina and D. Popova-Gorelova

105. Shock-frozen beams of biomolecules and nanoparticles for single particle imaging
A. D. Estillore, J. He, L. Worbs, S. Kiran Peraval, A.K. Samanta and J. Küpper

106. Theoretical description of time- and momentum resolved photoelectron spectroscopy probing excited-state dynamics in molecular systems at FELs
M. Reuner, K. Baumgärtner, M. Scholz and D. Popova-Gorelova

107. The Centre for Molecular Water Science - CMWS
C. Goy, S. Bari, F. Lehmkühler and M. Schnell

108. Controlling Fragmentation of the Acetylene Cation in the Vacuum-Ultraviolet via Transient Molecular Alignment
L. Varvarezos, J. Delgado-Guerrero, M. Di Fraia, T.J. Kelly, A. Palacios, C. Callegari, A.L. Cavalieri, R. Coffee, M. Danailov, P. Decleva, A. Demidovich, L. DiMauro, S. Düsterer, L. Giannessi, W. Helml, M. Ilchen, R. Kienberger, T. Mazza, M. Meyer, R. Moshammer, C. Pedersini, O. Plekan, K.C. Prince, A. Simoncig, A. Schletter, K. Ueda, M. Wurzer, M. Zangrando, F. Martín and J.T. Costello

109. Development of X-ray mirrors for PAL-XFEL using differential deposition
J. Kim

110. Effects of antimicrobial SPLUNC1 peptide derivatives on efficacy, toxicity, and membrane interations
T. Jakkampudi, Q. Lin, S. Mitra, A. Vijai, W. Qin, A. Kang, J. Chen, E. Ryan, R. Wang, Y. Gong, F. Heinrich, Y. Peter Di and S. Tristram-Nagle

111. X-ray optics for nanometer imaging
J.L. Dresselhaus, M. Prasciolu, H. Fleckenstein, N. Ivanov, M. Zakharova, H.N. Chapman and S. Bajt

112. NFFA European piolet (NEP)
J. Dwivedi, T.F. Keller and A. Stierle

113. Correlative spectro-microscopy to follow the oxidation of PtRh core-shell nanoparticles
J. Dwivedi, L. Bachmann, A. Jeromin, T. F Keller and A. Stierle

114. Time-Delay and Chirp Compensation of Soft X-ray Pulses in the Water Window
C. Braig, C. Seifert and A. Erko

115. An X-ray compound reflection zone plate at 8.3 keV
H. Löchel, S. Vadilonga, C. Braig, A. Firsov, A. Svintsov, M. Brzhezinskaya, M. Wojcik, A. Macrander, L. Assoufid and A. Erko

116. Time-resolved Pair Distribution Function Measurements Resolving Ultrafast Structural Dynamics in $CuIr_2S_4$
J. Griffiths, A. Flavia, S. Marks, L. Wu, P. Evans, S. Boutet, V. Esposito, A. Tadesse, J. Mitchell, D. Keen, M. Dean, S. Billinge, E. Bozin and I. Robinson

117. Surface correlations of femtosecond laser excited Al-coated multilayers observed by grazing-incidence x-ray scattering
L. Randolph, M. Banjafar, T. Yabuuchi, C. Baehtz, E. Brambrink, M. Bussmann, N. P. Dover, S. Göde, G. Jakob, L. Huang, Y. Inubushi, J. Koga, A. Kon, M. Makita, N. Mamiko, M. Paulus, A. Pelka, T. R. Preston, C. Rödel, J.-P. Schwinkendorf, Y. Sentoku, K. Sueda, T. E. Cowan, M. Kläui, T. Kluge, C. Gutt and M. Nakatsutsumi

118. Fabrication of X-Ray Gratings by Grey-Tone Electron-Beam Lithography and Thermal Oxidation of Silicon
N. Samadi, V. Guzenko and C. David

119. Dependence of the damage threshold on the in-situ temperature in materials under X-ray irradiation
N. Medvedev, Z. Kuglerová, M. Makita, J. Chalupský and L. Juha

120. Robust Ptychographic X-ray Speckle Tracking with Multilayer Laue lenses
N. Ivanov, J.L. Dresselhaus, J. Carnis, M. Domaracky, H. Fleckenstein, C. Li, T. Li, M. Prasciolu, O. Yefanov, W. Zhang, S. Bajt and H.N. Chapman

121. Imaging Ultrafast Chemical Dynamics
S. Trippel, I. Vinklárek, D. Koulentianos, H. Bromberger, A. Samartsev, W. Jin, M.S. Robinson, M. Singh, N. Vadassery and J. Küpper

122. Slip competition and rotation suppression in tantalum and copper during dynamic uniaxial compression
P. G. Heighway and J. S. Wark

123. Damage of alkene polymers under FEL irradiation
N. Nikishev and N. Medvedev

124. Bragg Coherent Modulation Imaging for Highly Strained Nanocrystals
J. Zhao, I. Vartaniants and F. Zhang

125. X-ray photon correlation spectroscopy (XPCS) as a use case for DAPHE4NFDI
A. Tosson, S. Timmermann, N. Das Anthuparambil, M. Dargasz and C. Gutt

126. On the feasibility of Time-resolved Powder X-ray diffraction of Macromolecules with low-flux laboratory based ultrafast X-ray sources
K.P. Khakurel

127. Ultrafast non-thermal melting of ice - from transient crystalline plasma to anisotropic melting
I. Dawod, K. Patra, S. Cardoch, O. Grånäs, H.O. Jönsson, A.V. Martin, J. Binns, J.A. Sellberg, A.P. Mancuso, N. Timneanu and C. Caleman

128. Speeding up X-ray-matter molecular dynamics simulation tool XMDYN with tree algorithms
M. Stransky, Z. Jurek, R. Santra, A. P. Mancuso and B. Ziaja

129. HMC Hub Matter
Luigia Cristiano, Gerrit Günther, Markus Kubin, Oonagh Mannix, Özlem Özkan, Gabriel Preuß, Mojeeb Rahman Sedeqi, Vivien Serve and Pascal Walter

130. Exploring biomolecular properties in the gas phase by using advanced light sources
L. Pille, L. Schwob, B. Oostenrijk, J. Leroux, A. Nair and S. Bari

131. Using electrospray ionization and tandem mass spectrometry to study the structure and dynamics of biomolecules
A. Nair, L. Schwob, J. Leroux, L. Pille, B. Oostenrijk, A. Kotobi, C. Mahecha and S. Bari

132. The EuPRAXIA photon beams: ultra-bright light pulses for imaging and spectroscopy
F. Stellato on behalf of the EuPRAXIA collaboration

133. State Localization Perspective of Ionization Potential Depression
T. Gawne, P. Hollebon, G. Perez-Callejo, O. Humphries, J. Wark and S. Vinko

134. Using molecular dynamics to characterise the vaporisation of an x-ray heated metal near its critical temperature
D. Peake, P. Heighway and J. Wark

135. Under Pressure: High-Pressure Biology with MacCHESS at Cornell High Energy Synchrotron Source
J. Wierman, S. Meisburger, R. Gillilan, Q. Huang, Z. Wang and J. Ruff

136. XAS reference database under DAPHNE4NFDI
A. Gaur, S. Paripsa, F. Förste, D. Doronkin, W. Malzer, C. Schlesiger, J.-D. Grunwaldt, B. Kanngießer and D. Lützenkirchen-Hecht

137. Large scale sputter deposition at DESY - magnetic multilayers, targets, x-ray and laser optics
K. Schlage, A. Panchwanee, A. Siemens, M. Ramin Moayed, C. Adolff, L. Bocklage, J. Lütjens and R. Röhlsberger

138. Laser absorption and x-ray radiation in microstructured Ti targets heated by short-pulse relativistically intense laser pulses
X. Pan, S. Sander, M. Šmíd, L. Huang, T. Kluge, V. Bagnoud, E. Brambrink, J. Colgan, T. Ebert, D. Hartnagel, M. Hesse, J. Hornung, A. Kleinschmidt, P. Perez-Martin, A. Neukirch, K. Philipp, G. Schaumann, A. Tebartz, B. Zielbauer, M. Roth and K. Falk

139. Challenges in the production of next generation optical elements with e-beam lithography
A. Fernández Herrero, S. Rehbein, A. Teichert, C. Braig, G. Gwalt, T. Krist, A. Erko and F. Siewert

140. Accurate data quality evaluation for serial crystallography
M. Galchenkova and O. Yefanov

141. Smart chips scanning for serial crystallography
M. Galchenkova, J. Mayer, A.R. Mashhour, P.Y.A. Reinke, H.N. Chapman and O. Yefanov

142. Ultrafast solvation dynamics of aqueous Cl, Br and I with optical and X-ray pump-probe method
Z. Nurekeyev, M. Sekkal, K. Kubicek and C. Bressler

143. Serial Femtosecond Crystallography with Deep Learning
D. Pennicard, H. Graafsma, S. Pala, R. Setty, V. Rahmani and S. Nawaz

144. Theoretical modeling of XFEL irradiated matter: from molecules to bulk systems
Z. Jurek, S. Banerjee, B. Richard and R. Santra

145. Chemical effects on the dynamics of organic molecules irradiated with high intensity x-rays
S. Banerjee, Z. Jurek, M. Muhammad Abdullah and R. Santra

146. Structural Dynamics Of Molecules With X-ray Spectroscopy And Simulations
L. Inhester

147. Efficient, pulse-train-based generation of high-energy, multicycle THz pulses for THz-driven electron acceleration and manipulation.
N.H. Matlis, Z. Zhang, C. Rentschler, Ü. Demirbas, M. Youssef, M. Pergament and F.X. Kärtner

148. Low-temperature cryostats for scientific applications
G. Yakopov, A. Goikhman and M. Yakopov

149. Inert gas glove boxes for scientific applications in particular for Li-ion battery production
D. Melnikov, A. Goikhman, G. Yakopov and M. Yakopov

150. Critical Step in the HCl Oxidation Reaction over single-crystalline CeO_{2-x}(111): Oxygen-Induced Site Change of Surface Chlorine
V. Koller, A. Spriewald-Luciano, S.M. Gericke, A. Larsson, C. Sack, A.Preobrajenski, E. Lundgren and H. Over

151. Electronic states in Moiré superlattices of TMDCs
C.H. Sharma, P. Zhao, J. Schmidt, L. Tiemann, M. Prada, L. Bußß, N. Wind, M. Scholz, F. Diekmann, T. Taniguchi, K. Watanabe, A.D. Pandey, A. Stierle, K. Rossnagel and R.H. Blick

152. Optical Sensing using Incoherent Diffractive Imaging
T. Wollweber and K. Ayyer

153. UV and Mid-IR Photo-induced Dissociation Dynamics of Solvated (Bio)Molecular Complexes
M. Singh, M.S. Robinson, H. Bromberger, J. Onvlee, S. Trippel and J. Küpper

154. Research opportunities in photon science at the ELI Beamlines user facility
M. Precek, B. Angelov, S. Espinoza, M. Kloz, M. Krikunova, E. Klimesova, M. Rebarz, A. Zymakova and J. Andreasson

155. Valley selectivity in soft x-ray spectroscopy of monolayer transition metal dichalcogenides: Femtosecond XAS as a novel probe of topological properties of 2-dimensional systems
A. Geondzhian, A. Rubio and M. Altarelli

156. Calculations of molecular excited states using neural networks
Á. Fernández-Corral, Y. Saleh, A. Yachmenev and J. Küpper

157. Bulk plasma temperature determination in high intensity laser solid interaction by time resolved optical shadowgraphy
L. Yang, L. Huang, S.Assenbaum, C. Bernert, I. Goethel, T. Kluge, M. Rehwald, X. Pan, U. Schramm, J. Vorberger, K. Zeil and T. E. Cowan

158. Microsecond time-resolved pink beam serial crystallography
S. Günther, A. Tolstikova, M. Galchenkova, O. Yevanov, P. Reinke, H. Chapman, R. Henning, M. Levantino and A. Meents

159. 3D structure determination with 3 MeV relativistic electrons
A. Rodrigues, V.Hennicke, M.Hachmann, W. Brehm, S. Thekku Veedu, J. Meyer, P. Reinke, L. Melo Costa, K. Bustos, M. Bartelmess, T. Pakendorf, H. Delsim Hashemi, K. Flöttmann and A. Meents

160. A comparative study on the photodissociation of gas-phase peptides in the VUV and soft X-ray regimes with a special focus on the influence of the methionine residue
S. Dörner, L. Schwob, K. Schubert, K. Atak, M. Girod, L. MacAleese, C. L. Pieterse, M. Timm, C. Bülow, V. Zamudio-Bayer, J. T. Lau, T. Schlathölter, S. Techert and S. Bari

161. Full-field x-ray fluorescence spectromicroscopy
P. Meyer, J. Soltau and T. Salditt

III.4 PETRA III

162. GINIX II – biomedical x-ray tomography for PETRA IV
M. Osterhoff, B. Hartmann, P. Luley, M. Sprung and T. Salditt

163. Crystal harvesting and HT ligand screening experiments P11 user lab: increasing your odds using the Crystal Shifter
S.D. Chatziefthymiou, H. Taberman, G. Pompidor, A. Gruzinova, J. Song and J. Hakanpää

164. Effects of X-ray dose and dose rate on structure and dynamics of egg white protein gels
S. Timmermann, N. Das, A. Girelli, N. Begam, M. Kowalski, S. Retzbach, M. Senft, M. Akhundzadeh, H. Poggemann, M. Moron, A. Hiremath, D. Gutmüller, M. Dargasz, Ö. Öztürk, M. Paulus, F. Westermeier, M. Sprung, A. Ragulskaya, F. Zhang, F. Schreiber and C. Gutt

165. Visualizing Exsolved Nanoparticles by Anomalous X-ray Scattering Methods
P. Inangha and S. Mascotto

166. Time-resolved GIWAXS investigations of slot-die coated quantum dot thin-film materials
M. Reus, L.K. Reb, A. Krifa, D. Kosbahn, Q.A. Akkerman, A. Biewald, M. Schwartzkopf, A. Chumakov, S.V. Roth, J. Feldmann, A. Hartschuh and P. Müller-Buschbaum

167. LVP station at P61B: In situ high-pressure studies using synchrotron white-beam
R. Farla, S. Bhat, S. Ma, C. Lathe, K. Spektor, A. Neri, L. Man, A. Chanyshev, S. Sonntag, T. Katsura, U. Haeussermann and H. Kohlmann

168. Upgrading the High-Energy Beamline P21.1 at PETRA III
K. Köhler, A. Dippel, M. von Zimmermann, A. Mirone and B. Winkler

169. MyoSAX - Exploring muscle function in disease and health
A. Hessel

170. Temperature-induced morphology changes at the organic-metal interface: effects on the structure, electronic and thermoelectric performance
B. Sochor, Y. Bulut, M. Betker, A.L. Oechsle, S. Schraad, C.R. Everett, C. Harder, T.-Y. Huang, A. Le Brun, T. Laarmann, P. Müller-Buschbaum and S.V. Roth

171. Current Status and Capabilities of the Extreme Conditions Beamline P02.2 at PETRA III
H.P. Liermann, K. Glazyrin, N. Giordano, T. Fedotenko, M. Wendt, S. Wenz, I. Schwark, J.-T. Roehr and A. Ehnes

172. Planing for the Extreme Conditions Time Resolved XRD & Imaging Microscope (ExTReM) at PETRA IV
H.P. Liermann and K. Glazyrin

173. Aberreation-corrected multilayer Laue lenses
F. Seiboth, A. Kubec, A. Schropp, S. Niese, P. Gawlitza, J. Garrevoet, V. Galbierz, S. Achilles, S. Patjens, M. E. Stuckelberger, C. David and C.G. Schroer

174. Development of CoRDIA: a Detector for next-generation X-ray Sources
A. Marras

175. Toward efficient real-time computation of autocorrelation functions for X-ray photon correlation spectroscopy using FPGAs
S. Frücht, C. Gutt, T. Kenter, R. Lammert, C. Plessl, M. Sprung, H.-G. Steinrück, A. Rehman Tareen and F. Westermeier

176. Probing redox and structural dynamics of V species in V-W-TiO_2 catalysts by operando X-ray emission spectroscopy
D. Doronkin, L. Zheng, F. Benzi, M. Casapu and J.-D. Grunwaldt

177. Iron as an energy source for a climate-neutral circular economy
L. Braun, V. Marchuk, D. Doronkin and J.-D. Grunwaldt

178. Construction of a fast non-linear X-ray shutter system
M. Kowalski, M. Sprung, M. Paulus, D. Weschke, M. Ziolkowski, S. Timmermann and C. Gutt

179. Tunable mesoporous and optoelectronics properties of zinc titanate films using sol-gel technique
Y. Li, N. Li, S. Yin, C. Harder, Y. Bulut, A. Vagias, S.V. Roth and P. Müller-Buschbaum

180. Self-organized structures in/on In/CuPcFx metal-organic interface.
O.V. Molodtsova, D.V. Potorochin, A.N. Chaika and V.Yu. Aristov

181. Layer-by-layer sequential production of graphene on an epitaxial SiC(001) layer grown on a Si(001) substrate
V. Aristov, A. Chaika, D. Potorochin and O. Molodtsova

182. Cochleate structures for drug delivery investigated by SAXS
P. Garidel and S. Funari

183. Development of a photoelectron spectrometer for Hard X-ray photon diagnostics at the European XFEL
J. Laksman, F. Dietrich, J. Liu, T. Maltezopoulos, M. Planas, W. Freund, S. Francoual and J. Grünert

184. X-ray emission setup at P01 to study the electronic structure of iron-bearing compounds *in situ* at high pressure and high temperature
N. Thiering, C. Albers, R. Sakrowski, J. Kaa, G. Scholz, J. Savelkouls, W. Morgenroth, M. Sundermann, H. Gretarsson, M. Wilke, M. Tolan and C. Sternemann

185. Giant Supramolecules Meet Synchrotron Radiation
A. Virovets, E. Peresypkina and M. Scheer

186. The High-Troughput Macromolecular Crystallography Beamline P11 at PETRA III
H. Taberman, C. Borges, S. Chatziefthymiou, E. Crosas, A. Gruzinov, B. Kistner, G. Pompidor, J. Song and J. Hakanpää

187. High Energy X-Ray Diffraction for Physics and Chemistry at beamlines P07 and P21.1 at PETRA III, DESY
I. Gjerlevsen Nielsen, O. Ivashko, P. Glaevecke, O. Gutowski, A.-C. Dippel and M. von Zimmermann

188. PERCIVAL: First users experiments
J. Correa, M. Mehrjoo, R. Battistelli, F. Lehmkühler, A. Marras, C. B. Wunderer, T. Hirono, V. Felk, F. Krivan, S. Lange, I. Shevyakov, V. Vardanyan, M. Zimmer, M. Hoesch, K. Bagschik, N. Guerrini, B. Marsh, I. Sedgwick, G. Cautero, L. Stebel, D. Giuressi, R.H. Menk, A. Greer, T. Nicholls, W. Nichols, U. Pedersen, P. Shikhaliev, N. Tartoni, H.J. Hyun, S.H. Kim, S.Y. Park, K.S. Kim, F. Orsini, F.J. Iguaz, F. Büttner, B. Pfau, E. Plönjes, K. Kharitonov, M. Ruiz-Lopez, R. Pan, S. Gang, B. Keitel and H. Graafsma

189. EASI-STRESS: Standardisation of Industrial Residual Stress Measurements
M. Thiry, D. Canelo-Yubero, E. Maawad, P. Staron, N. Schell, G. Abreu Faria, M. Sanchez-Poncela, J. M. Martinez and N. Zangenberg

190. The hydrothermal autoclave at beamline P65 - recent developments and research examples related to ore deposit formation
M. Borchert, M. Kokh, P. Valsera Moreno, M. Wilke, R. Al Abed, Ch. Schmidt, A. Loges, D. Testemale, W. Morgenroth and S. Klemme

191. In-situ investigation during gold HiPIMS deposition onto polymers
Y. Bulut, B. Sochor, J. Drewes, K. Reck, S. Liang, T. Guan, T. Strunskus, F. Faupel, P. Müller-Buschbaum and S.V. Roth

192. P66 beamline for VUV time- resolved spectroscopy
A. Kotlov, Y. Smortsova, O. Chukova, A. Kataev and I. Schostak

193. Small molecule crystallography beamline, P24
L. Noohinejad and M. Tolkiehn

194. Acoustic emissions detection of micro-cracks under high pressure and high temperature in a deformation large-volume apparatus
S. Ma, J. Gasc, S. Sonntag and R. Farla

195. X-RAYS meet NEUTRONS meet IONS meet ELECTRONS meet LASERS meet MAGNETS: COMBINED ACCESS TO MULTIPLE FACILITIES THROUGH EU PROJECT REMADEARI
M. Stuckelberger, C. Ossig, S. Facsko and B. Schramm

196. Evaluation and Recommendations for Electronic Laboratory Notebooks empowering FAIR Data Management
P. Jordt, W. Lohstroh and B. Murphy

197. Visualization of Strain Distribution in Gold|FeCoSiB coated ZnO Microstructures utilizing Bragg CDI
P. Jordt and R. Rysov and N. Wolff and S. Hrkac and S. Shree and D. Wang and R. Harder and C. Kübel and R. Adelung and O. Shpyrko and O. Magnussen and L. Kienle and B. Murphy

198. Mass Spectrometry Platform as Sample Delivery System for Gas-phase Protein SAXS Experiments
J.C.K. Kung, T. Damjanović, E. De Santis, E.G. Marklund, C. Coleman, T. Kierspel and C. Uetrecht

199. Lattice thermal expansion of as-grown GaAs nanowires due to optical excitation measured by X-ray pump-probe experiment
T. Anjum, F. Marín Largo, A. Al Hassan, R. Prasad Giri, L. Petersdorf, V. Salehi, M. Rössle, B. Murphy, O. Brandt, L. Geelhaar and U. Pietsch

200. Stability of the Fe_3O_4 $(\sqrt{2}\times\sqrt{2})$R45° surface in 0.1M NaOH probed by High-Energy Surface Diffraction
J. Bunge, D. Grumelli, O. Fehrs, T. Fuchs, L. Jacobse, J. Stettner, A. Stierle and O. Magnussen

201. A versatile chemical vapor synthesis reactor for in situ X-ray absorption spectroscopy and X-ray scattering
S. Joshi, M. A. Schroer, A. Levish, M. Stepponat and M. Winterer

202. Raytracing for Beamline Alignment
J. Seltmann, K. Bagschik, M. Hoesch, M. Huang and F. Scholz

203. Active layer aging for the fabricating durable perovskite solar cells with improved reproducibility
Y. Zou and P. Müller-Buschbaum

204. In-situ observation of growth mechanisms during printing of 2D perovskite film
K. Sun, R. Guo, L. F. Huber, M. A. Reus, J. Zhou, M. Schwartzkopf, S.V. Roth and P. Müller-Buschbaum

205. Investigation of Lipid Nanoparticles for Therapeutic Compound Delivery Using Small-Angle X-ray Scattering
B. Angelov, M. Drechsler and A. Angelova

206. PETRA III: P03/MiNaXS - current status and future plans
J. Rubeck, M. Schwartzkopf, A. Chumakov, B. Sochor, A. Davydok, C. Krywka, S. Roth and J. Neumann

207. Multi-beam X-ray ptychography using coded probes
M. Lyubomirskiy, F. Wittwer, M. Kahnt, F. Koch, A. Kubec, K.V. Falch, J. Garrevoet, M. Seyrich, C. David and C.G. Schroer

208. P25: Beamline for Applied Bio-Medical Imaging, Powder Diffraction and Innovation
K. Spiers, N. Thielen, C. Qiu, B. Struth, M. Etter, A. Schoekel, A. Burkhardt, G. Falkenberg and H.-C. Wille

209. A grazing incidence diffraction setup for Langmuir trough experiments at the high-resolution diffraction beamline P08 at PETRA III
C. Shen, R. Kirchhof and F. Bertram

210. PETRA III: Advanced Applications of Synchrotron Radiation
O.H. Seeck, H.-C. Wille and C. Schroer

211. The Powder Diffraction and Total Scattering Beamline P02.1 at PETRA III, DESY
V. Baran, H. Jeppesen, A.S.J. M'endez, A. Schökel, T. Schoof, M. Wendt, S. Wenz and M. Etter

212. Timepix4 readout for experiments at synchrotrons and FELs
J. Correa, A. Ignatenko, D. Pennicard, S. Lange, S. Fridman, S. Smoljanin and H. Graafsma

213. Three-dimensional virtual histology of human heart-forming organoids based on phase-contrast x-ray tomography
K. Komorowski, J. Reichmann, L. Drakhlis, J. Frost, R. Zweigerdt and T. Salditt

214. The high resolution diffraction beamline P08
F. Bertram, R. Kirchhof, C. Shen, A.B. Dey, B. Bharatiya and J. Zhang

215. Phase relations in NH_3-defective NH_3-H_2O mixtures at high pressure
A. Mondal, R. J. Husband, H.-P. Liermann and C. Sanchez-Valle

216. Structure of Water and Ice Under Confinement in Periodic Mesoporous Organosilicas (PMOs)
N. Giesselmann, S. Schwake, P. Lenz, T. Simon, W. Jo, C. Koehn, N. Striker, M. Froeba and F. Lehmkühler

217. 3d virtual histology reveals pathological alterations of cerebellar granule cells in multiple sclerosis
J. Frost, B. Schmitzer, M. Töpperwien, M. Eckermann, J. Franz, C. Stadelmann and T. Salditt

218. Combined X-ray Emission Spectroscopy and Raman Spectroscopy of supercooled water
C. Goy, F. Trinter, R. Bauer, M. Caresana, Y. Chang, M. Harder, S. C. Hoevelmann, A. Kalinin, S. Lalithambika, Y. Zhong and R. Grisenti

219. Photoinduced disulfide bond cleavage and recombination in a copper-sulfur complex studied with Cu and S K-edge pump-probe X-ray absorption spectroscopy
M. Naumova, A. Tayal, J. Ortmeyer, B. Grimm-Lebsanft, S. Buchenau, A. Kalinko, S. Canton, G. Smolentsev and T. Huthwelker

220. Investigation of the Hot Deformation Behavior in VDM® Alloy 780 by In-situ High-energy X-ray Diffraction
M. Fritton, F. Kümmel, A. Kirchmayer, A. Stark, M. Hafez Haghighat, B. Gehrmann, S. Neumeier and R. Gilles

221. Photo-induced structural changes in phospholipid monolayers and vesicles containing azobenzene-glycoconjugates
S. Hövelmann, J. Warias, K. Hansen, J. Kuhn, S. Reinheimer, E. Dieball, R. Giri, L. Petersdorf, N. Hayen, A. Sartori, P. Jordt, C. Shen, F. Reise, T. Lindhorst, O. Magnussen and B. Murphy

222. Pump probe investigations of structural dynamics at the liquid-vapour interface of salt solutions
L. Petersdorf, S. Hövelmann, R. Giri, N. Hayen, K. Hansen, P. Jordt, A. Sartori, M. Greve, F. Bertram, O. Magnussen and B. Murphy

223. SAXS/WAXS imaging at the SAXSMAT beamline: status and future perspectives
A.L.C. Conceicao, S. Pfeffer and S. Haas

224. Adsorption of spike amino acids, asparagine and cysteine, on the surface of model catalyst TiO_2
M. Blanco Garcia, M. Kohantorabi, M. Wagstaffe, M. Tehrani, S. Dolling, A. Stierle and H. Noei

225. Biological SAXS on the P12 beamline and covid-related application
D. Soloviov, A. Gruzinov, M. Schroer, M. Graewert, C. Jeffries, D. Franke, D. Svergun and C. Blanchet

226. Coherence Applications Beamline P10
F. Westermeier, N. Das A, V. Kartik, Z. Ren, W. Roseker, R. Rysov, D. Weschke, H. Xu and M. Sprung

227. XAS reference database under DAPHNE4NFDI
S. Paripsa, D. Lützenkirchen-Hecht, F. Förste, W. Malzer, C. Schlesiger, B. Kanngießer, A. Gaur, D. Doronkin, K. Kornetzky and J.-D. Grunwaldt

228. The SAXSMAT beamline P62: Small Angle X-ray Scattering Beamline for Materials Research
S. Haas, X. Sun, A. Conceicao and S. Pfeffer

229. Shape reconstruction of PtPd nanocatalysts investigated by Bragg CDI during methane oxidation
B. Wang, T.F. Keller, J. Schobe, S. Bernart, L. Bachmann, J. Dwived, A.D. Pandey, K.H. Ngoi, G. Hinsley, D. Lapkin, R. Ryzhov, M. Sprung, A. Stierle and I. Vartaniants

230. Dynamics and Timescales of Higher Order Correlations in Supercooled Colloidal Systems
N. Striker, I. Lokteva, M. Dartsch, F. Dallari, C. Goy, F. Westermeier, V. Markmann, S. C. Hövelmann, G. Grübel and F. Lehmkühler

231. pydidas: A software package to improve the user experience for diffraction data analysis
M. Storm, P. Staron and C. Krywka

232. WaveGate: fast and versatilex-ray chopper for sychrotron beams
D. Schmidt and P. Gaal

233. Stability of biobased coatings on textiles
L. Pluntke, C. Harder, S. Chen, I. Ribca, N. Kölpin, M. Oberthür, P. Müller-Buschbaum, M. Johansson and S.V. Roth

234. Real-time data processing for serial X-ray crystallography
T.A. White, T. Schoof, S. Yakubov, A. Tolstikova, V. Mariani, A. Henkel, B. Klopprogge, A. Prester, S. de Graaf, M. Galchenkova, O. Yefanov, J. Meyer, G. Pompidor, J. Hannappel, D. Oberthuer, J. Hakanpaa, M. Gasthuber and A. Barty

235. Cellulose-based recyclable efficient solar cells by ultrasonic spray process
S. Xiong, C. Harder, B. Sochor, P. Müller-Buschbaum and S.V. Roth

236. Machine Learning for the Automated Selection and Reconstruction of Multi-Modal Nanotomography Data of Bone-Implant Interfaces
B. Schacht, B. Zeller-Plumhoff, I. Greving and S. Frintrop

237. Exploring non-equilibrium processes in a heated egg yolk using coherent X-rays
N. Das Anthuparambil, A. Girelli, S. Timmermann, M. Kowalski, M. Akhundzadeh, S. Retzbach, M. D. Senft, M. Dargasz, D. Gutmüller, A. Hiremath, M. Moron, Ö. Öztürk, H.-Friederike Poggemann, A. Ragulskaya, N. Begam, A. Tosson, M. Paulus, F. Westermeier, F. Zhang, F. Schreiber, M. Sprung and C. Gutt

238. Layer by Layer Spray - Coating of Cellulose Nanofibrils and Lignin
S. Chen, C. Harder, I. Ribca, L. Pluntke, M. Oberthuer, M. Johansson, J. Navarro and S V. Roth

239. Bragg coherent X-ray diffraction imaging at P10 beamline
Z. Ren, H. Xu, R. Rysov, V. Kartik, D. Weschke, F. Westermeier and M. Sprung

240. next-generation Percival Mechanics
S. Rah, J. Correa, A. Marras, C.B. Wunderer, V.Vardanyan, F. Krivana, V. Felk, S. Lange, F. Okrent, I. Shevyakov, M. Hoesch, K. Bagschik, M. Zimmer, N. Guerrini, B. Marsh, I. Sedgwick, G. Cautero, D. Giuressi, R.H. Menk,h, G. Pinaroli, L. Stebel, A. Greer, T. Nicholls, U. Pedersen, N. Tartoni, H.J. Hyun, K.S. Kim, F. Orsini, A. Dawiec, F. Buettner, B. Pfau, R. Battistelli and H. Graafsma

241. Dose rate-dependent X-ray induced dynamics in dense antibody-protein solutions immunoglobulin G
M. Sayed Akhundzadeh, A. Girelli, S. Timmermann, N. Das Anthuparambil, M. Kowalski, N. Begam, A. Vladimirovna Ragulskaya, M. Reiser, H.-F. Poggemann, M. Senft, F. Westermeier, M. Sprung, F. Schreiber, F. Zhang and C. Gutt

242. Studying magnetism with x-ray standing waves - new experimental results
M. Kamiński, P. Pokhriyal, H. Schulz-Ritter, L. Bouchenoire, S. Francoual and M. Tolkiehn

243. The Swedish Materials Science Beamline (SMS) at PETRA III: In-line branch (P21.2)
U. Lienert, S. Gutschmidt, T. Baecker, Zoltan Hegedues and Malte Blankenburg

244. New developments in the software MagStREXS
P. J. Bereciartua, S. Francoual, W. Xie, C. Plueckthun and J. Rodríguez-Carvajal

245. Neodymium acetate as a contrast agent for x-ray phase-contrast tomography
J. Reichmann, T. Ruhwedel, W. Möbius and T. Salditt

246. sXRD study of copper-zinc-alumina (CZA) model systems under methanol synthesis conditions
E. Beck, V. Vonk, H. Noei and A. Stierle

247. Novel magnetic cellulose nanocomposite coating as a potentially flexible electronic material
A. Chumakov, K. Gordeyeva, C.J. Brett, D. Menzel, A.V. Riazanova, D. Soederberg and S.V. Roth

248. Effect of strain rate on slip activation in a Mg-Al alloy by in-situ 3DXRD
G. Zhu, A. Shabalin, U. Lienert and L. Wang

249. High pressure and low temperature single crystal diffraction capabilities at the Resonant Scattering and Diffraction beamline P09, DESY
C. Plückthun, J. Sears, P.J. Bereciartua, J. Bergtholdt, A. Ehnes, J. Geck, K Glazyrin, M. Kusch, H.-P. Liermann, L. Veiga and S. Francoual

250. Implementation of an environmental cell for in situ nanotomography of biological specimen at the imaging beamline P05
M. Nopens, I. Greving, S. Flenner, J. Lüdtke, M. Altgen, S. Heldner, H. Köhm, J. Beruda and A. Krause

251. Nanobeam Scanning 3D X-ray Diffraction Microscopy of a CdTe Solar Cell
A. Shukla, H. Stieglitz, J. Wright, H.F. Poulsen, A. Henningson, M. Stuckelberger, L. Besley, C. Baur, C. Krywka, A. Davydok and J. W. Andreasen

252. In situ X-ray diffraction and imaging beamline P23
D. Novikov, A. Khadiev and M. Nentwich

253. HIKa - Hierarchical Imaging Karlsruhe at Desy
C. Sato Baraldi Dias, M. Czyzycki, D. Novikov and T. Baumbach

254. Insights into physico-chemical properties of Pt/Rh gauze catalysts during industrial ammonia oxidation using hard X-ray microscopy
S. Das, M. Stuckelberger, J. Pottbacker, S. Jakobtorweihen, R. Horn and T. L. Sheppard

255. Bimetallic exsolution of Ni-Fe nanoparticles from perovskite oxides: an insight on mechanistic aspects through in-situ XANES and synchrotron XRD for tailoring catalytic selectivity
F. Colombo, A. Tsiotsias, B. Rudolph, B. Ehrhardt, M. Goula and S. Mascotto

256. Structure and Stability of Methane and Methane Hydrates at Planetary Conditions
K. Mohrbach, A. Mondal, R. Husband, H.-P. Liermann and C. Sanchez-Valle

257. Combined phase contrast imaging and diffraction at extreme conditions
E. Ehrenreich-Petersen, E.F. O'Bannon, J. Hagemann, D.T. Sneed, D.J. Campbell, B. Massani, T. Engler, R. Husband, K. Glazyrin, T. Fedotenko, M. Wendt, S. Wenz, R.S. McWilliams, H.-P. Liermann and Zs. Jenei

258. Sub-micrometer focusing setup for high-pressure crystallography at the Extreme Conditions beamline at PETRA III
K. Glazyrin, S. Khandarkhaeva, T. Fedotenko, W. Dong, D. Laniel, F. Seiboth, A. Schropp, J. Garrevoet, D. Brückner, G. Falkenberg, A. Kubec, C. David, M. Wendt, S. Wenz, L. Dubrovinsky, N. Dubrovinskaia and H.-P. Liermann

259. Determination of structural parameters of mesocrystals formed by polymer-functionalized Au octahedral nanocrystals using AXCCA
S. Singh, D. Lapkin, F. Kirner, S. Sturm, T. Wiek, T. Gemming, A. Lubk, D. Assalauova, A. Ignatenko, A. Khadiev, D. Novikov, E.V. Sturm and I.A. Vartanyants

260. In-operando studies of piezoelectric HfO2 on III-V semiconductor nanostructured devices
S. Singh, Z. Ren, N. Zaiats, I. Vartaniants and A. Mikkelsen

261. Toward high energy resolution in soft X-ray resonant inelastic X-ray scattering using standard photoemission setups
J.O. Schunck, J. Buck, M. Kalläne, S.R. Kruse, R.Y. Engel, S. Marotzke, M. Scholz, S.K. Mahatha, M.-J. Huang, H.M. Rønnow, G. Dakovski, M. Hoesch, K. Rossnagel and M. Beye

262. Structural Investigation of Exsolved Nanoparticles from Thin Films by X-Ray Scattering
E. Fezai, J. K. Kim, M. Schawrtzkopf, W. C. Jung and S. Mascotto

263. Unveiling temperature-induced changes in the protein-protein interactions of cryoprotected Lysozyme solutions
M. Filianina, M. Bin, M. Reiser, S. Berkowicz, H. Li, S. Timmermann, K. Amann-Winkel, C. Gutt and F. Perakis

264. P61A: Materials science experiments with a high energy white beam at PETRA III
G. Abreu Faria, P. Staron and M. Müller

265. Precipitation kinetics in Al alloy 7050 studied by SAXS, WAXS, and numerical modeling
S. Henninger, J. Herrnring, P. Staron, B. Klusemann and M. Müller

266. Development of X-ray compound refractive lenses for synchrotron beamlines
H. van der Velde, D. Spinov, M. Lyubomirskiy, F. Seiboth, C.G. Schroer, W.T.E. van den Beld, M.D. Ackermann and I.A. Makhotkin

267. Revealing Packing Behavior of 3D Binary Mesocrystals through Angular X-ray Cross-Correlation Analysis (AXCCA)
K.H. Ngoi, D. Lapkin, F. Kirner, G. Hinsley, S. Sturm, L. Saric, V. Vuksan, S. Singh, R. Rysov, M. Sprung, S. Park, E. Sturm and I. Vartaniants

268. Resolving the 3D Structure of Au Colloidal Mesocrystals by Coherent X-ray Diffractive Imaging
G. Hinsley, R. Rysov, F. Kirner, D. Lapkin, S. Singh, D. Assalauova, M. Sprung, S. Sturm, E. Sturm and I. Vartaniants

269. X-ray microscopy - an illumination correction
T. Engler, J. Hagemann, M. Trabs and C.G. Schroer

270. Spatial electronic structure of 2H-Hf_2S
C.-H. Min, A. Nierhauve, M. Kalläne, J. Buck and K. Rossnagel

271. Muscle Ankyrin Repeat Protein 1 (MARP1) alters sarcomere protein structures in mammalian skeletal muscle via titin association
M.N. Kuehn, W. Ma, S.W. Han, J. Fleming, O. Mayans, T. Irving, W.A. Linke and A.L. Hessel

272. Towards reconstructing conformational dynamics from protein crystal diffuse scattering
P. Mazumder and K. Ayyer

273. Quantitative Phase-Contrast Imaging at the Micro CT Beamlines P05 and P07
M. Riedel, F. Beckmann, J. U. Hammel, J. Moosmann, F. Wilde, M. Busse and J. Herzen

274. Quantitative, size dependent characterization of mRNA nanoparticles by in line coupling of asymmetrical flow field-flow fractionation with small angle x-ray scattering
C. Wilhelmy, M.A. Graewert, R. Drexel, F. Meier, B. Kolb, C. Blanchet, T. Nawroth, T. Bacic, J. Schumacher, D. Svergun, T. Klein, H. Haas and P. Langguth

275. Phase retrieval in X-ray holographic imaging: beyond the homogeneous object approximation
J. Lucht, S. Huhn, L.M. Lohse and T. Salditt

276. New instrumentation at the chemical crystallography beamline P24
M. Tolkiehn, P. Pokhriyal, L. Noohinejad, H. Schulz-Ritter and C. Paulmann

277. High spatial resolution X-ray diffraction for highly absorbing samples at P06, PETRA III
P. Chakrabarti, A. Wildeis, M. Hartmann, R. Brandt, M. Stückelberger, G. Fevola, C. Ossig, R. Döhrmann, V. Galbierz, K.V. Falch, J. Garrevoet, G. Falkenberg and P. Modregger

278. Data analysis workflow for high-energy grain-resolved 3D x-ray diffraction
A. Shabalin, G. Zhu, J. Hektor, J. Gustafson, B. Neding and U. Lienert

279. Coherent X-ray Scattering Reveals Nanoscale Fluctuations in Hydrated Proteins
M. Bin, M. Reiser, M. Filianina, S. Berkowicz, S. Das, S. Timmermann, W. Roseker, R. Bauer, J. Öström, A. Karina, K. Amann-Winkel, M. Ladd Parada, F. Westermeier, M. Sprung, J. Möller, F. Lehmkühler, C. Gutt and F. Perakis

280. Recent Developments in X-Ray Nanotomography at P05
S. Wirtensohn, S. Flenner, I. Greving and J. Herzen

281. Real-Time Processing Deep Learning Pipeline for Peak Localization and Indexing of GIWAXS Data
V. Starostin, V. Munteanu, L. Pithan, F. Bertram, D. Gavran, A. Gerlach, A. Hinderhofer and F. Schreiber

282. Object initialization for improved ptychography
F. Wittwer, D. Brückner and P. Modregger

283. Correlative imaging of biodegradable Mg-based alloys using in situ SRnanoCT and electron microscopy techniques
Jan Reimers, Huu Ch'anh Trinh, Marta Lipinska-Chwalek, Regine Willumeit-Römer, Joachim Mayer, Imke Greving and Berit Zeller-Plumhoff

284. Advanced methods for phase retrieval in Phase-Contrast tomography.
D. Hailu, T. Jentscht, V. Kulvait and J. Moosmann

285. *In Operando* Soft X-Ray Photoemission Spectroscopy of TMDC Devices
A. Nierhauve, M. Kalläne, J. Buck, T. Zimmermann, Z. Geng, C. Sharma, R. Venturini, C. Zhang, F. Schwierz, M. Ziegler and K. Rossnagel

286. Structural and dynamic analysis of Human Insulin by X-Ray Photon Correlation Spectroscopy
N. Das Anthuparambil, M. Kowalski, M. Dargasz, O. Koutit, C. Gutt and S. Timmermann

287. Nuclear forward scattering in a mono-modal x-ray waveguide
L.M. Lohse

288. Phase-Contrast Tomography of Organoids
J. Alfken, M.P. Zafeiriou and T. Salditt

289. Time-resolved structural changes in hybrid perovskites under illumination
I. Zaluzhnyy, L. Pithan, A. Hinderhofer, R. Rysov, F. Paulus and F. Schreiber

290. Pulsed laser deposition setups development for thin films in situ growth & investigations
P. Prokopovich, A. Dolgoborodov, E. Fatyanov and A. Goikhman

291. X-ray lens transfocators. Precision refractive optics focusing devices
A. Dolgoborodov, P. Prokopovich, E. Fatyanov and A. Goikhman

292. Coherent correlation imaging for resolving fluctuating states of matter
C. Klose, F. Büttner, W. Hu, C. Mazzoli, K. Litzius, R. Battistelli, I. Lemesh, J.M. Bartell, M. Huang, C.M. Günther, M. Schneider, A. Barbour, S.B. Wilkins, G.S.D. Beach, S. Eisebitt and B. Pfau

293. Towards fast 2d x-ray photon correlation spectroscopy of magnetic domains with the PERCIVAL detector
C. Klose, M. Schneider, B. Pfau, S. Eisebitt, D. Ksenzov, S. Timmermann, C. Gutt, C. Wunderer, T. Hirono, A. Marras, J. Correa, M.-J. Huang, M. Hoesch, K. Bagschick, F. Lehmkühler, R. Gruber, K. Raab, M. Kläui, A. Yaroslavtsev and H. Dürr

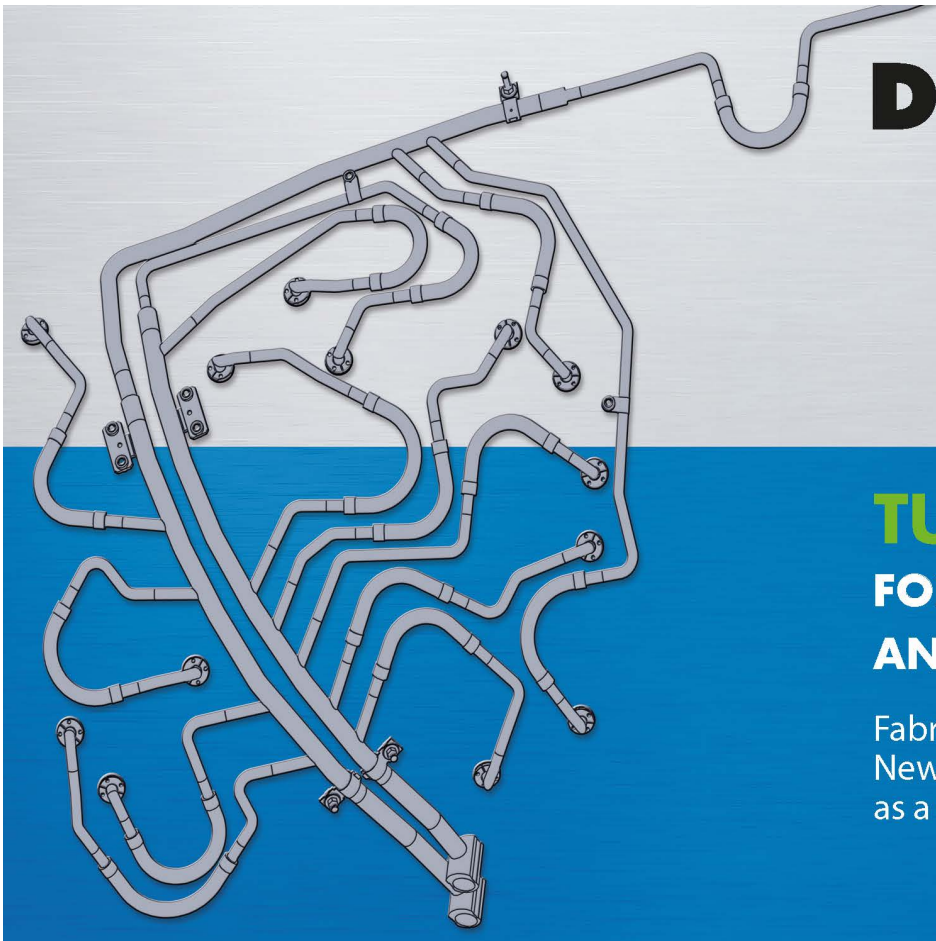

DOCKWEILER

connecting flow to purity

TUBE SYSTEMS

FOR CLEAN MEDIA AND VACUUM TECHNOLOGY

Fabrication of complex geometries
New: tube connection ZeroCon - as tight as a weld seam

Cooling loop for In Vessel-components of Wendelstein 7-X
CAD-Model courtesy of IPP

Dockweiler AG
An der Autobahn 30
19306 Neustadt-Glewe, Germany
Phone: +49 38757 58 0, info@dockweiler.com
www.dockweiler.com

294. Neurodegenerative diseases in the aging population: 3D x-ray phase contrast images analysis of epiphyseal calcification
O. Junemann, M. Fratini, I. Bukreeva and A. Cedola

295. Three-dimensional image segmentation of human olfactory bulb structures using deep learning approach
I. Bukreeva, O. Junemann, A. Cedola and M. Ftratini

296. Development of a wavefront analysis platform for online beam characterization at next-generation synchrotron beamlines.
A. Sharma, F. Seiboth and C. Schroer

297. Developing real time coherence analysis platform at next-generation synchrotron beamlines
A. Sharma, F. Seiboth and C. Schroer

298. Simulation of Tomography Experiments with Phasecontrast X-ray at PETRA III
T. Jentschke, F. Otte, J. Moosmann, T. Farago and M. Müller

299. Depth resolved magnetic structure investigation of thin magnetic films using nuclear resonant scattering
A. Panchwanee, K. Schlage, L. Bocklage, S. Velten, A.I. Chumakov, O. Leupold, S. Sadashivaiah, I. Sergeev and R. Röhlsberger

300. Phase Retrieval from 2-Dimensional Nuclear Resonant Scattering spectra
A. Negi, L. Bocklage, L.M. Lohse, S. Sadashivaiah, O. Leupold, I. Sergeev, G. Meier, C, Brandt and R. Röhlsberger

301. Room temperature in-situ synchrotron creep of Fe-based shape memory alloy
M.J. Oza, C. Leinenbach, A. Stark, P.B. Vila and M. Shahverdi

302. Instrumentation for time-resolved synchrotron X-ray diffraction studies of adsorption-induced switching in crystalline nanoporous solids
V. Bon, A. Khadiev and D. Novikov

303. Spatiotemporal design of Metal-Organic Frameworks by tuning of the crystal size and the composition of the metal node
V. Bon, H. Miura, N. Busov, A. Khadiev, D. Novikov and S. Kaskel

304. Investigating the influence of applied loads on degrading Mg-10Gd
B. Hindenlang, F. Wieland, D. Tolnai, F. Wilde and R. Willumeit-Römer

305. New highly luminescent lanthanide metal-organic frameworks based on 2,4,6-tri-(phenylene-4-phosphonic acid)-s-triazine (H6PPT) ligand
K. Papathanasiou, F. Steinke, E.E.S. Teotonio, H. Terraschke and N. Stock

306. Unraveling the Spatial Distribution of Catalytic Non-Cubic Au Phases in a Bipyramidal Microcrystallite by X-ray Diffraction Microscopy
C. Sow, A. Sarma, A. Schropp, D. Dzhigaev, T.F. Keller, C.G. Schroer, M.K. Sanyal and G.U. Kulkarni

307. New luminescent hybrid organic-inorganic Lanthanide based Dipicolinato materials
P.L. Djonwouo, J. Ströh, G. Doungmo, E. Teotonio, W. Bensch, C. Näther and H. Terraschke

308. Resolving x-ray wave mixing processes
C. Boemer, F. Kerker, D.Krebs and N. Rohringer

309. FeCoSiB metallic glass annealing studied by in situ X-Ray Total Scattering
N. Hayen, P. Jordt, L. Thormählen, M. Mewes, A.-C. Dippel, O. Gutowski, N. Wolff, L. Kienle, O.M. Magnussen and B.M. Murphy

310. Photoemission Microscopy with Hard X-rays: HAXPEEM at P22
C. Wiemann and C. M. Schneider

311. Influence of XUV radiation on the ion-molecule chemistry in the ionosphere
S. Reinwardt, I. Baev, P. Cieslik, K. Baev, T. Buhr, A. Perry-Sassmannshausen, S. Schippers, A. Müller, F. Trinter, J. Viefhaus and M. Martins

312. Photoelectron Circular Dichroism from Aqueous-Phase Biomolecules
M. Pugini, D. Stemer, K. Mudryk, L. Tomanik, S. Malerz, F. Trinter, T. Buttersack, U. Hergenhahn, I. Wilkinson, S. Thuermer, P. Slav´ivcek, B. Winter and G. Meijer

313. Photo-emission spectroscopy on resistive switching processes in the ferromagnetic oxide La0.7Sr0.3MnO3
D. Gogoi, C. Wiemann and C.M. Schneider

314. Pushing the limit - Recent advances in intracellular crystallography
J. Boger, R. Schönherr and L. Redecke

315. Operando XAS Tomography for rapid 3D characterization of Mo-catalysts for oxidative dehydrogenation of ethane
S. Alizadehfanaloo, V. Murzin, B. Wollak, S. Das, R. Horn, C. G. Schroer, T. Sheppard and A. Schropp.

316. Nanotube Research at P23: from powders to single nanotube analysis
A. Khadiev, M.B. Sreedhara, R. Tenne and D. Novikov

317. Dynamically controllable resonant x-ray optics and interferometry via mechanically induced refractive-index control
M. Gerharz, D. Lentrodt, L. Bocklage, K. Schulze, C. Ott, R. Steinbrügge, O. Leupold, I. Sergeev, G. Paulus, C. H. Keitel, R. Röhlsberger, T. Pfeifer and J. Evers

318. In situ CO and partial CH_4 oxidation on Pd NP/CeO_2/YSZ model catalyst
J. Schober, S. Dolling, E. Beck, M. Kao, M. Creutzburg, D. Novikov, T. Keller, V. Vonk and A. Stierle

319. Influence of dye-doping on the nanostructure of the highly efficient PM6:Y6 solar cells
E. Erbes, C. Harder, B. Sochor, S. Frenzke, N. Biswas, J. Rubeck, M. Schwartzkopf, V. Körstgens, P. Müller-Buschbaum, S.V. Roth and S. Techert

320. Full-field nanotomography: Time resolution and in situ applications
S. Flenner, J. Hagemann, E. Longo, M. Storm, S. Wirtensohn and I. Greving

321. Machine learning denoising of high resolution nanotomography data
S. Flenner, S. Bruns and I. Greving

322. Dose-efficient in-situ imaging of gold nanocage formation using near-field ptychography
J. Voss, K. Stachnik, S. Roeper, M. Astrand, L. Grote, S. Niese, P. Gawlitza, F. Wittwer, S.-A. Hussak, H. Ohlin, D. Koziej, C. Schroer, U. Vogt and A. Schropp

323. Self-optimization of reconstruction parameters enables online view for holographic in-situ experiments
J. Dora, J. Hagemann, S. Flenner, I. Greving, C. Schroer and T. Knopp

324. ASPHERE III: Soft X-ray (spin-)ARPES endstation at P04, PETRA III
H. Bentmann, J. Buck, F. Diekmann, T. Figgemeyer, B. Geldiyev, P. Kagerer, J. Kähler, M. Kalläne, L. Kipp, A. Nierhauve, S. Marotzke, C.-H. Min, H. Orio, A. Philippi-Kobs, T. Riedel, J. Schusser, C. Harihara Sharma, M. Ünzelmann, N. Wind, T. Zimmermann, F. Reinert and K. Roßnagel

325. Effects of phase composition on luminescent characteristics of $La_{1-x}Dy_xVO_4$ nanoparticles
O. Chukova, S.A. Nedilko, S.G. Nedilko and T. Voitenko

326. Ultrafast dynamics of OCS
W. Jin

327. Caseinolytic Protease P and Boronate Derivatives: Revisiting Structure-Function Features of Protein Modulation
B.A. França, V. Srinivasan, H. Rohde and C. Betzel

328. Control and Timing System of a synchrotron X-ray chopper for time resolved experiments
U. Ristau, V. alnati, D.Jahn, J. Meyer and S. Fiedler

329. X-ray phase contrast tomography of excised cochleae
J.J. Schaeper, C. Kampshoff, L. Roos, D. Keppeler, B.J. Wolf, T. Moser and T. Salditt

330. Sprayed nanocellulose-based silver nanowire transparent electrodes
M. Betker, C. Harder, E. Erbes, J. Heger, A. E. Alexakis, B. Sochor, Q. Chen, M. Schwartzkopf, A. Chumakov, P. Müller-Buschbaum, K. Schneider, S. Techert, L.D. Söderberg and S.V. Roth

331. Influence of the imbibition of colloids through the optical and wetting properties of porous CNF layers
C. Harder, M. Betker, A. Alexakis, Y. Bulut, S. Xiong, E. Erbes, B. Sochor, K. Goordeyeva, M. Gensch G. Pan, H. Zhong, M. Reus, Q. Chen, A. Chumakov, J. Rubeck, V. Körstgens, M. Schwartzkopf, A. Jeromin, T. Keller, D. Söderberg, E. Malmström, P. Müller-Buschbaum and S. Roth

332. Sample changer and fixed-chi sample stage for P24 EH1
C. Schäfer, C. W. Lehmann and C. Paulmann

333. How the skeleton adapts to an extremely short lifespan: Revealing bone matrix and mineral properties in the shortest-lived vertebrate model: the killifish
I.A.K. Fiedler, F.N. Schmidt, E.M. Wölfel, A. Davydok, K. Jähn-Rickert, D.R. Valenzano and B. Busse

334. Bone matrix mineralization and mineral particle thickness in breast cancer-cell induced bone lesions
J. Krug, I.A.K. Fiedler, A. Davidok, S. Conrad, G. Furesi, H. Hemmatian, J.D. Kuhlmann, M. Rauner, B. Busse and K. Jähn-Rickert

335. Variation of the relative humidity to study protein flexibility
P. Reinke, S. Günther, J. Lieske, W. Ewert, S. Falke, A. Creon, S. Thekku Veedu, O. Yefanov, V. Hennicke, J. Meyer, T. Pakendorf, P. Fischer and A. Meents

336. Current status of the P06 Beamline
J. Garrevoet, D. Brueckner, K.V. Falch, V. Gelbierz and G. Falkenberg

337. Second Order Phase Transition and Stabilizing CH···H and CH···S Interactions in Naphthyl End-Capped Bithiophene at 3.5 GPa
N. Giordano, S. Guha, B. Stewart, J. Kjelstrup-Hansen and M. Knaapila

338. Influence of geometry on residual stress in additively manufactured aluminium alloy parts
M.-A. Nielsen, P. Staron, E. Maadwad, S. Bodner, F. Resch, J. Keckes and M. Müller

339. Ribavirin at high pressure
B. Tiwari, N. Giordano, S. Parsons and H.-P. Liermann

340. Inside mycelium – synchrotron radiation and image processing to unveil the three-dimensional growth of filamentous fungal pellets
H. Müller, J. Hammel and H. Briesen

341. The achromatic X-ray lens and its recent developments
P. Qi, U. Sanli, G. Rodgers, M.-C. Zdora, A. Kubec, A. Diaz, M. Humbel, G. Schulz, J. Garrevoet, M. Scheel, T. Weitkamp, B. Müller, C. David and J. Vila-Comamala

342. Inelastic X-ray Scattering at the Dynamics Beamline P01
H. Gretarsson, M. Sundermann, F.-U. Dill, S. Mayer and I. Sergeev

IV Author Index (Submitting author only)

(Submitting author and poster number)

List of Exhibitors at the Industry Exhibition during poster sessions (Bldg. 80d)

ADL GmbH
Aerotech GmbH
Agilent Technologies Deutschland GmbH
ALCA TECHNOLOGY SRL
Allectra GmbH
Amplitude
attocube systems AG
Beckhoff Automation GmbH & Co. KG
Best Fluidsysteme GmbH
Carl Zeiss SMT GmbH
Createc Fischer & Co. GmbH
Cryoandmore GbR
Cycle GmbH
DECTRIS Ltd.
Dockweiler AG
FMB Berlin & Oxford
greateyes GmbH
HAMAMATSU PHOTONIK Deutschland GmbH
Hiden Analytical Europe GmbH
Hositrad Vacuum Technology
Huber Diffraktionstechnik | AXO DRESDEN
Hy-Lok D Vertriebs GmbH
Incienta Technologie GmbH
JJ X-Ray
Johann Fischer Aschaffenburg GmbH & Co. KG
Just Vacuum GmbH
Kleindiek Nanotechnik
Leybold GmbH
mechOnics ag
MEWASA AG
OELZE GmbH
Pfeiffer Vacuum GmbH
Phytron GmbH
PINK GmbH Vakuumtechnik
ProxiVision GmbH
SmarAct GmbH
Spetec GmbH
SYMETRIE
UHV Design
Vacuum FAB srl
VAQTEC SRL
VAT Germany GmbH
XRnanotech GmbH
X-Spectrum GmbH